Investigation of the interaction of DAD1-LIKE LIPASE 3 (DALL3) with Selenium Binding Protein 1 (SBP1) in Arabidopsis thaliana

Dervisi, I.; Valassakis, C.; Agalou, A.; Papandreou, N.; Podia, V.; Haralampidis, K.; ... ; Roussis, A.

Plant Science 291 (2020) 110357

Contents lists available at ScienceDirect

Plant Science

journal homepage: www.elsevier.com/locate/plantsci

Investigation of the interaction of DAD1-LIKE LIPASE 3 (DALL3) with Selenium Binding Protein 1 (SBP1) in *Arabidopsis thaliana*

Irene Dervisi[a], Chrysanthi Valassakis[a], Adamantia Agalou[b,1], Nikolaos Papandreou[c], Varvara Podia[a], Kosmas Haralampidis[a], Vassiliki A. Iconomidou[c], Vassili N. Kouvelis[d], Herman P. Spaink[b], Andreas Roussis[a,*]

[a] Department of Botany, Faculty of Biology, National & Kapodistrian University of Athens, 15784, Athens, Greece
[b] Institute of Biology, Leiden University, Leiden, the Netherlands
[c] Department of Cell Biology and Biophysics, Faculty of Biology, National & Kapodistrian University, 15784, Athens, Greece
[d] Department of Genetics and Biotechnology, Faculty of Biology, National & Kapodistrian University of Athens, 15784, Athens, Greece

ARTICLE INFO

Keywords:
SBP1
Selenium Binding Protein 1
DALL3
Phospholipase

ABSTRACT

Phospholipase PLA_1-Iγ2 or otherwise DAD1-LIKE LIPASE 3 (DALL3) is a member of class I phospholipases and has a role in JA biosynthesis. AtDALL3 was previously identified in a yeast two-hybrid screening as an interacting protein of the Arabidopsis Selenium Binding Protein 1 (SBP1). In this work, we have studied AtDALL3 as an interacting partner of the Arabidopsis Selenium Binding Protein 1 (SBP1). Phylogenetic analysis showed that DALL3 appears in the PLA1-Igamma1, 2 group, paired with PLA1-Igammma1. The highest level of expression of *AtDALL3* was observed in 10-day-old roots and in flowers, while constitutive levels were maintained in seedlings, cotyledons, shoots and leaves. In response to abiotic stress, DALL3 was shown to participate in the network of genes regulated by cadmium, selenite and selenate compounds. DALL3 promoter driven GUS assays revealed that the expression patterns defined were overlapping with the patterns reported for *AtSBP1* gene, indicating that *DALL3* and *SBP1* transcripts co-localize. Furthermore, quantitative GUS assays showed that these compounds elicited changes in activity in specific cells files, indicating the differential response of DALL3 promoter. GFP::DALL3 studies by confocal microscopy demonstrated the localization of DALL3 in the plastids of the root apex, the plastids of the central root and the apex of emerging lateral root primordia. Additionally, we confirmed by yeast two hybrid assays the physical interaction of DALL3 with SBP1 and defined a minimal SBP1 fragment that DALL3 binds to. Finally, by employing bimolecular fluorescent complementation we demonstrated the *in planta* interaction of the two proteins.

1. Introduction

Phospholipases are a group of enzymes that hydrolyze phospholipids and are categorized based on their positional specificity toward phospholipid substrates. In plants, it is known that there are phospholipases A (PLA), C (PLC) and D (PLD) while phospholipases B have not been identified [1,2]. These enzymes are involved in a wide range of cellular functions such as cellular regulation, lipid metabolism, membrane homeostasis, stress responses and cell signaling [1,2].

The PLA superfamily contains a broad range of enzymes that are designated with Greek letters and have been classified into three subtypes: PLA_1 and PLA_2, which hydrolyse acyl groups from the *sn*-1 and *sn*-2 positions of phospholipids respectively, and patatin-like PLAs (PAT-PLA) all exhibiting activity towards both positions [1]. Furthermore, the molecules mediated by PLAs act as secondary signal messengers that mediate cell elongation, gravitropism, anther dehiscence, biosynthesis of jasmonic acid and defense [3]. It is noteworthy that these enzymes play a significant role in important applications of food and biotechnology industries, such as degumming of vegetable oils, diary, baking or egg yolk treatment and biodiesel production [4,5].

Specifically, PLA_1 proteins hydrolyze phospholipids and produce 2-acyl-lysophospholipids and fatty acids [6] and they are involved in a wide range of cellular functions including jasmonic acid biosynthesis [7,8], defense signaling induced by ultraviolet (UV) radiation [9], cell and tissue growth [10], onset of senescence [11], storage lipid accumulation [11,12] and shoot gravitropism [13]. All PLA_1 proteins

* Corresponding author.
E-mail address: aroussis@biol.uoa.gr (A. Roussis).
[1] Current address: Developmental Biology, Biomedical Research Foundation Academy of Athens, Soranou Ephessiou 4, 11527, Athens, Greece.

https://doi.org/10.1016/j.plantsci.2019.110357
Received 26 June 2019; Received in revised form 18 November 2019; Accepted 21 November 2019
Available online 23 November 2019
0168-9452/

contain a Gly-X-Ser-X-Gly (GXSXG) motif and a catalytic triad (Ser, Asp, His) and have molecular weights of about 45 − 50 kDa [1,14,15]. This superfamily can be further divided into five groups I, II, III, lecithin:cholesterol acyltransferase-like PLA_1 (LCAT- PLA_1) and PA- PLA_1 [1,3]. However, classes I, II and III are usually referred to, as PLA_1 phospholipases [1].

In the Arabidopsis genome 12 isoforms of PLA_1 family have been identified [3], one of which is DEFECTIVE IN ANTHER DEHISCENCE1 (DAD1) and the other 11 proteins are homologues of it. These proteins are further grouped into the three previously mentioned classes (I,II,III) based on the presence of N-terminal stretches and sequence similarities in the catalytic region [3,8,16]. Class I, contains seven proteins, that have been shown to be localized in the chloroplasts [16] and are involved in jasmonic acid (JA) biosynthesis. Class II consists of four proteins and class III of one protein, which are predicted to be localized in the cytosol and mitochondria, respectively [3,8,16]. These lipases possess the α/β hydrolase fold [17] and the lipase active site is characterized by an active center. This, is composed of a serine (nucleophile), an aspartic (acidic residue) and a histidine and by the GXSXG consensus sequence, including the serine residue of the catalytic triad [8,16].

Analytically, the α/β fold is generally composed of a central, parallel β-sheet of eight beta- strands, with only the second strand antiparallel. Another characteristic is the presence of disulfide bridges that given the enzyme stability, are often important for the catalytic activity. The tetrahedral intermediate formed during the catalytic mechanism of lipases is stabilized by the presence of hydrogen bonds with two amino acids form the so-called lipase oxyanion hole. These amino acids stabilize the intermediate through hydrogen bonds between their backbone amide proton and the oxygen of the substrate carbonyl group [18,19].

Phospholipase PLA_1-Iγ2 or otherwise DAD1-LIKE LIPASE 3 (DALL3, AT2G30550) is a member of class I phospholipases and has a role in JA biosynthesis as its knockout halved the JA levels in untreated leaves [20]. Wounded plants produce high amounts of JA, and this phospholipase is induced upon wounding, however, it is also expressed in unwounded leaves [7,20,21]. Other experiments using JA-biosynthetic and JA-response mutants revealed that wound induction of DALL3 is regulated in a COI1-independent and JA-independent manner [20]. Furthermore, AT2G30550 has two isoforms generated by alternative splicing from which AT2G30550.2 encodes the functional protein [16]. Seo and colleagues [16] also showed that this phospholipase has strong PLA_1 activity and can hydrolyze Phosphatidylcholine (PC), Monogalactosyldiacylglycerol (MGDM), Diglycosyl diacylglycerols (DGDG) and Triacylglycerol (TAG). Microarray experiments showed that DALL3 expression increases after abiotic and biotic stress [22] and may play a role in the Pathogen-associated Motif Patterns (PAMPs)-response pathway [23].

AtDALL3 was previously identified in a yeast two-hybrid screening as an interacting protein of the Arabidopsis Selenium Binding Protein 1 (SBP1) [24]. In Arabidopsis, SBP1 could be considered as a general stress-responsive gene as revealed by microarray analyses [25–29], while in rice, plants overexpressing *OsSBP* showed enhanced resistance to a virulent strain of rice blast fungus as well as to rice bacterial blight possibly by increasing plant sensitivity to endogenous defense responses [30–32]. *in vitro* binding assays have shown that in Arabidopsis SBP1 participates in a novel protein network consisting of at least SBP, a NADP-dependent glyceraldehyde-3-phosphate dehydrogenase (GAPDH) and a fructose-bisphosphate aldolase (FBA) [24]. Additionally, SBP1 also interacts with the PICOT-containing glutaredoxins AtGRXS14 and AtGRXS16 [33]. Finally, it has been suggested that SBP gene family may participate in the mechanisms that sense redox imbalance [34]. In this work, we have studied AtDALL3 as an interacting partner of the Arabidopsis Selenium Binding Protein 1 (SBP1). Both proteins are involved in plant stress responses and we propose that they are part of a novel interaction network active in abiotic stress induced by selenium and cadmium compounds as well as in wounding.

2. Material and methods

2.1. Plant material and growth conditions

Arabidopsis thaliana ecotype Columbia (Col-0) and transgenic Arabidopsis plants harbouring prDALL3-DELs::GUS and 35S::DALL3::eGFP expression cassettes were used in the present study. Seeds were initially stratified for two days at 4 °C, surface sterilized for two min in 75 % (v/v) ethanol, 4 min in 25 % (v/v) bleach and washed with sterile distilled water. Afterwards, they were transferred to soil (Postground P, Klasmann-Deilmann, Geeste, Germany) or plated on Petri dishes containing solid half-strength MS medium (Duchefa Biochemie, Haarlem, Netherlands) [35] supplemented with 0.05 % MES (2-(N-morpholino) ethanesulfonic acid) (Sigma-Aldrich, St. Louis MO, USA) pH 5.7, Gamborg's B5 vitamins, a micronutrient mixture (Duchefa Biochemie, Haarlem, Netherlands), 2 % (w/v) sucrose and 1.2 % (w/v) agar (Difco Laboratories, Detroit, MI, USA). The seeds were germinated and grown in a plant growth chamber under long-day conditions at 22 °C (16 h photoperiod).

2.2. Yeast two-hybrid assays

10-days seedling cDNA was used to amplify *DALL3*. The set of oligonucleotides used for the amplification was designed based on the nucleotide sequence available in the NCBI database for the accession number NM_128607, and properly modified to include unique restriction sites. The forward primer (5′- GCTTCTCACATATGGCGGCTATTC CTTCC- 3′) contained the *NdeI* restriction site where the reverse primer (5′-GCGTGAATTCTTAACAAGGATGATCAAGACGG-3′) the *EcoRI* site. For the amplification, LongAmp *Taq* DNA Polymerase (New England Biolabs, Beverly, MA, USA) was used. After amplification, the full length *DALL3* cDNA was cloned into the pJET1.2 vector (Thermo Scientific™). To construct the bait vector, the pJEI1.2/DALL3 was digested with *NdeI/EcoRI* and then cloned to the same restriction sites of the $pGBKT_7$ fused with the Gal4 binding domain. The deletions of SBP1 (DEL1-8) from the full length *At*SBP1 cDNA were cloned in the *NdeI/BamHI* sites of pGADT7 vector fused with the activation domain of Gal4, except AtSBP1DEL8 for which domain swapping was performed, essentially as described by Valassakis et al. [33]. For the yeast transformation and interaction study we followed the Matchmaker™ GAL4 Two-Hybrid System 3 protocol, (Takara-Clontech, Kyoto, Japan) and the yeast strain used was *Saccharomyces cerevisiae* SG335 (*MATa trp1-901, leu2-3, 112, ura1-52, his3-200, gal4Δ, gal80Δ, GAL2-ADE2, LYS2::GAL1-HIS3, met2::GAL7lacZ*). Yeast two-hybrid screening was performed as described by Agalou et al. [24].

2.3. Treatment of plants with chemical compounds and wounding

Arabidopsis seeds plated on half-strength MS medium were grown vertically for 4 days. At this point, young seedlings were transplanted onto plates containing half-strength MS medium plus 150 μM selenite (Na_2SeO_3; Sigma-Aldrich), 150 μM sodium selenate (Na_2SeO_4; Alfa Aesar, Karlsruhe, Germany) and 150 μM cadmium chloride ($CdCl_2$; Fluka Honeywell) and grown under the conditions mentioned above for 4 days. The chemicals used for the treatments were maintained in 50 mM stock solutions in distilled water. Seedlings transplanted onto plates containing only half-strength MS medium were used as controls. Roots from 8-days old control and treated seedlings were collected, weighted, frozen in liquid nitrogen and stored in −80 °C for use in real-time quantitative RT-PCR analysis, while intact plants were collected for histochemical and fluorometric GUS assays. For the wounding study we followed the protocol described by Ruduś and colleagues [20].

2.4. RNA extraction, cDNA synthesis and gene expression analysis

The transcript levels of *AtDALL3* gene were analyzed using total RNA following the procedure described by Oñate-Sanchez and Vicente-Carbajosa [36]. RNA samples were treated with DNAse I (Biolabs, Ipswich, England) according to the manufacturer's instructions. The RNA purity and quantity were checked by electrophoresis in a 0.8 % w/v agarose gel. Following electrophoresis, the RNA was stained with ethidium bromide (100 μg l^{-1}, Sigma-Aldrich) and visualized under UV light.

First-strand cDNA synthesis was performed using 1 μg of total RNA as template and SMART MMLV RT (Takara-Clontech, Kyoto, Japan). For quantitative (q) RT-PCR, KAPA SYBR® FAST qPCR Master Mix (2x) Kit (Kapa Biosystems, Woburn, MA, USA) were used according to the manufacturer's instructions. The reactions were performed in a thermal cycler (Applied Biosystems, Foster City, CA, USA). Ubiquitin 10 (UBQ10) and Protein Phosphatase 2 (PP2A) were used as housekeeping controls for normalization. Gene expression experiments were performed in triplicate. The relative expression levels of target genes and SD values were calculated using the $2^{-\Delta\Delta CT}$ Livak method [37], and statistically significant differences in expression between samples were detected using a *t*-test. Those with $P < 0.05$ were considered statistically significant. SigmaPlot statistical software (SigmaPlot 10.0) was used to analyze statistical significance. Variance analysis was performed using one-way ANOVA. All PCR products were separated by electrophoresis in 1.2 % agarose gels and visualized under UV light after staining with ethidium bromide (100 g L^{-1}). The primers used for amplification were as follows: Ubiquitin 10, UBQ10 (At4g05320): RLT-UBQ10-F (5′-AGAAGTTCAATGTTTCGTTTCATGTAA -3′) RLT-UBQ10-R (5′- GAACGGAAACATAGTAGAACACTTATTCA -3′), DAD1-Like Lipase 3, DALL3 (At2g30550): RLT-DALL3-F (5′- CGTGATATCGCGATTGCG TGG -3′) RLT-DALL3-R (5′- GTCGCCGTGTTCTTCCACTAAC -3′), Serine/Threonine Protein Phosphatase 2A, PP2A (At1g69960): RLT-PP2A-F (5′- TGATCCAGATGACCGATGCG -3′) RLT-PP2A-R (5′- GAGT GGTTTCGGGTTCGACT -3′).

2.5. Construction of vectors for plant transformation

The promoter sequences of DAD1-Like Lipase 3 were obtained from TAIR. The *DALL3* (AT2G30550) promoter deletions from *Arabidopsis thaliana* (L.) Heyn. (ecotype Columbia) genomic DNA were PCR amplified using specific pairs of primers. These primers introduced *EcoRI* and *NcoI* restriction enzyme sites (9 bp length each) at the 5′ and 3′ ends of the amplified sequences, respectively. PCR was performed using LongAmp *Taq* DNA Polymerase (New England Biolabs, Beverly, MA, USA) for 30 cycles. PCR products were separated by electrophoresis on 0.8 % agarose gels, visualized under UV light after staining with ethidium bromide (100 μg l^{-1}) and purified using a Nucleospin Gel and PCR Clean up kit (Macherey-Nagel, Düren, Germany). All plasmids were purified using Nucleospin Plasmid kits (Macherey-Nagel, Düren, Germany). The first pair of primers (PR-DALL3-F, 5′-CGCGAATTCACT TGAGTTTCTTGAACCATATGC-3′ and PR-DALL3-R, 5′-GCCGCCATGGT TGAGAAGCTTCAAAAGC-3′) amplified a 3.116bp region before the transcription site. This PCR product it was first cloned in pJET1.2 vector (Thermo Sientific™) and afterwards pJET1.2/PR-DALL3 was used for the amplification of the five 5′- deletions. The primes used for the five detions were: PR-DALL3-DEL1-F (5′- GCTAAAGAATTCGGTACATCCG CACATGT -3′) PR-DALL3-DEL2-F (5′- CTCCTATCGAATTCTTACTTTCT CTTGTGTGC -3′) PR-DALL3-DEL3-F (5′- GAAAATTGAATTCGCAACCT CCTAGCTAAGTGAC -3′) PR-DALL3-DEL4-F (5′- GGATCCATGAATTCT GATCTGTACCAGATTGC -3′) PR-DALL3-DEL5-F (5′- GTTGAGGAATTC AATTCTCTTGTCACTTACCGG -3′) keeping the same reverse primer. All PCR products were first cloned in pJET1.2 vector and then cloned into the *EcoRI/NcoI* sites of pCambia 1301 binary vector upstream of the β-glucuronidase (GUS) reporter gene, generating the following plasmid constructs: pCambia 1301-prDALL3::GUS, pCambia 1301-prDALL3-DEL1::GUS, pCambia 1301-prDALL3-DEL2::GUS, pCambia 1301-prDALL3-DEL3::GUS, pCambia 1301-prDALL3-DEL4::GUS, pCambia 1301-prDALL3-DEL5::GUS.

For the localization study we constructed 35S::DALL3::eGFP plants. Firstly, the gene *AtDALL3* was amplified from pJEI1.2/DALL3 using the following primers: F-DALL3-pSAT, 5′-GATCTCAGAGGAGGAATTCCAT ATGGCGGC-3′ and R-DALL3-pSAT, 5′- CCCCGGGAACTCTTGACAAGG ATG-3′. This PCR product cloned in $pGBKT_7$ with restriction sites *EcoRI/XmaI*. Then with *EcoRI/SalI* digestion from $pGBKT_7$ cloned in $pSAT_6$-eGFP-N by cloning the open reading frame, forming $pSAT_6$-DALL3::eGFP. The 35S::DALL3::eGFP cassette was cloned in the binary vector pPZP-RCS2-ntpII (CD3-1061) with the restriction site *PI-PspI*.

2.6. Plant transformation

Competent cells of *Agrobacterium tumefaciens* strain GV3101 were transformed with the aforementioned vectors by the general freeze thaw method, as described by An et al. [38]. The transformed bacteria were then used for the stable transformation of Arabidopsis (Columbia-0) plants via the floral dip method [39].

2.7. Histochemical and fluorometric GUS assays

GUS histochemical analysis was performed in 7-day seedlings as well as 4–5 weeks old flowers and seedlings. For GUS staining, the samples were prefixed in 90 % acetone for 30 min at 4 °C and washed twice with 100 mM sodium phosphate buffer pH 7.0 containing 0.1 M $K_3Fe(CN)_6$, 0.1 M $K_4Fe(CN)_6$ and 10 % (v/v) Triton X-100. The samples were then incubated at 37 °C overnight in reaction buffer containing 0.9 mg ml^{-1} 5-bromo-4-chloro-3-indolyl β-D-glucuronide sodium salt as substrate (Melford Laboratories Ltd., Ipswich, England) in the same buffer [40]. Samples were cleared in graded ethanol series (20 %, 35 %, 50 %, 70 % 90 %, 100 % v/v) for 30 min each and immersed in 90 % (v/v) ethanol for 30 min. Finally, the samples were kept overnight at room temperature in an aqueous chloral hydrate clearing solution containing glycerol and stored in the same solution. The samples were examined with a Zeiss Axioplan microscope (Zeiss, Oberkochen, Germany) equipped with a differential interference contrast (DIC) optical system and an Axiocam MRc5 digital camera (Zeiss) or with a Zeiss Stemi 2000-C stereomicroscope equipped with a Jenoptik ProgRes3 (Jenoptik, Jena, Germany) digital camera. Fifteen to twenty independent T2 lines were stained for each construct. More than 10 seedlings were examined from each line.

For the quantification of the enzymatic activity we followed the protocols described by Jefferson et al. and Gallagher et al. [40,41]. Total protein quantification was performed by the Bradford Assay [42]. Standard curves were prepared with 4-MU (Sigma). Specific GUS activity is shown in units of nanomoles 4-MU produced per milligram of protein per minute. All measurements were repeated three times on eight to 12 independently transformed plants from each construct.

2.8. Protoplast analysis

The construct of $pSAT_6$-DALL3::eGFP was described previously. For the $pSAT_4$-DALL3::nCerulean-N_1 construct, *AtDALL3* was isolated from $pGBKT_7$/DALL3 with *EcoRI/SalI* ends and cloned in the open reading frame of $pSAT_4$-nCerulean-N_1. *AtSBPs* were cloned in pSAT1-cCFP-N_1 with *EcoRI/XmaI* as it has been described in Valassakis et al. [33] forming $pSAT_1$-SBP1::cCFP-N_1, $pSAT_1$-SBP2::cCFP-N_1 and $pSAT_1$-SBP3::cCFP-N_1. For the isolation and transformation of mesophyll protoplasts we followed the Tape-Arabidopsis Sandwich method, as described by Wu and colleagues [43], while for the isolation of root protoplasts we used the protocol of Bargmann and Birnbaum [44]. The protoplasts were observed in a Zeiss Axioplan fluorescence microscope (Zeiss, Oberkochen, Germany), and photographs of each sample were taken using an Axiocam MRc5 digital camera (Zeiss) using the same

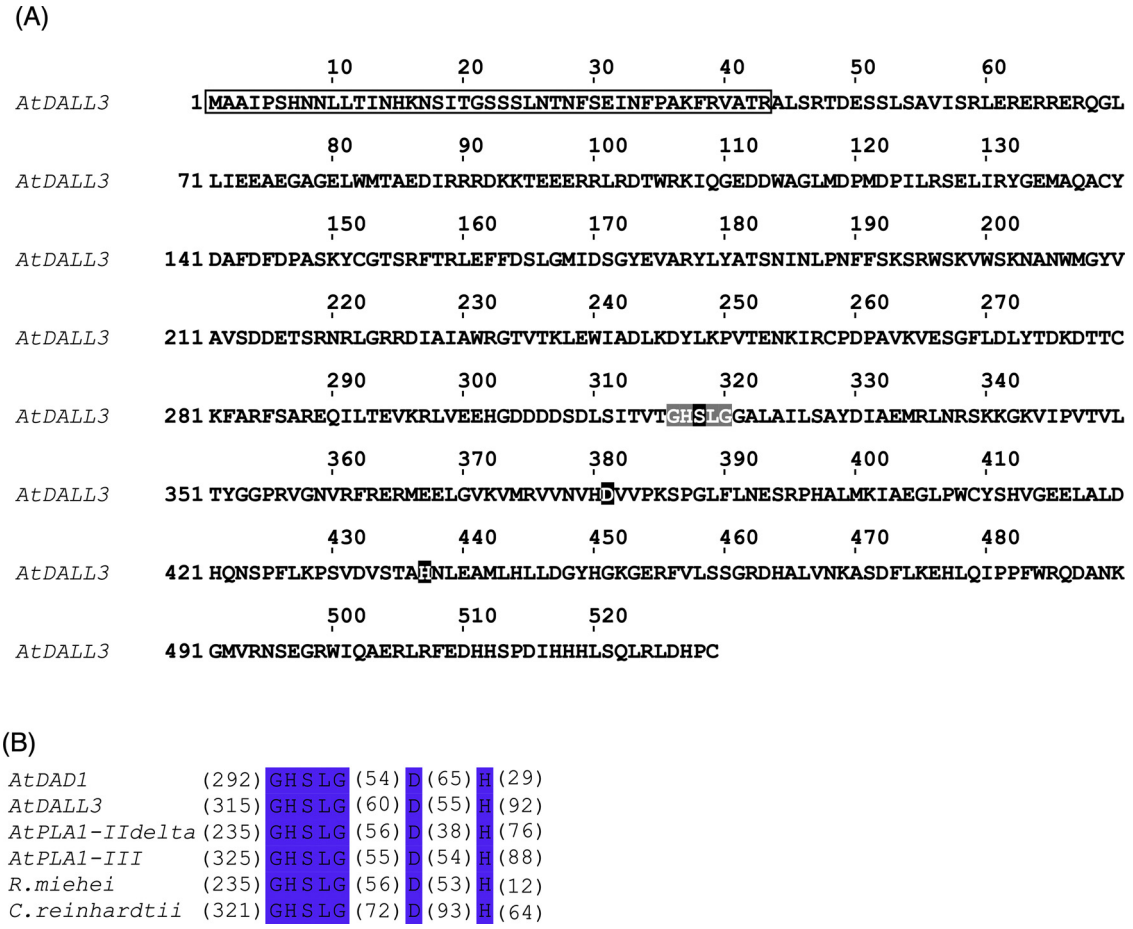

Fig. 1. Amino acid sequence and multiple protein alignment of *At*DALL3. (A) Linear sequence of *At*DALL3. The boxed area indicates the chloroplastic target peptide. Shaded amino acid residues represent the consensus motif GXSXG and the catalytic triad which is constituted by serine, aspartic acid and histidine residues. (B) Amino acid alignment in the catalytic region of *At*DALL3 and its homologues from *Chlamydomonas reinhardtii*, *Rhizomucor miehei* and *Arabidopsis thaliana* (*At*DAD1, *At*PLA1-IIdelta, *At*PLA1-III). Numbers in brackets indicate the number of amino acids. The residues are highlighted based on the identity, using JalView 2.10.5. (For interpretation of the references to colour in this figure legend, the reader is referred to the web version of this article.)

exposure time.

2.9. GFP imaging

To determine the cellular expression of the phospholipase we followed a propidium iodine (PI) staining as described by Prof. Philip N. Benfey's Laboratory (https://sites.duke.edu/benfey/protocols/). After dipping whole plants or dissected roots in PI (Sigma) Solution 10 μg ml^{-1}, we subsequently dipped them in double distilled water. Specimens were examined on a multiphoton confocal microscope Leica TCS SP8 MP (Wetzlar, Germany) equipped with an Argon laser (excitation lines at 458, 476, 488, 496, and 514 nm) and an IR MaiTai DeepSee Ti:Sapphire laser (Spectra-Physics, Santa Clara, CA, USA) for multiphoton applications. Images were acquired with the spectral detector of the microscope using appropriate emission wavelength ranges. For the detection of Green Fluorescence Protein excitation peak centered at about 488 nm, emission was 500 – 550 nm, while for PI excitation was at 591 nm and emission was in the range 590–700 nm. Acquisition was performed with the LAS X software (Leica Microsystems CMS GmbH, Wetzlar, Germany) using the same parameters (laser power, gain, pinhole, speed and analysis) for all specimens. Images were acquired as stacks for stomata and the root apex of 10–15 optical sections, while for root and lateral root of 60–75 optical sections with a Z-step of 1 μm.

2.10. Phylogenetic analysis

Phospholipases A1, members of the DAD1-like lipase family, were collected from 15 out of 59 different orders of Angiosperm, Bryophytes, Lycopods and a unicellular photosynthetic organism *Chlamydomonas reinhardtii* comprising a matrix of 146 proteins. These proteins were collected by BLASTp, firstly with DALL3 (Phospholipase A1-Igamma2, Q3EBR6.2) and then using the protein sequences of the members of DAD1 family [(Phospholipase A1-Ialpha1 (Q9MA46.1), Phospholipase A1-Ialpha2 (Q9SIN9.1), Phospholipase A1-Ibeta1 (DAD1, Q948R1.1), Phospholipase A1-Ibeta2 (O23522.2), Phospholipase A1-Igamma1 (Q941F1.2), Phospholipase A1-Igamma3 (Q9C8J6), Phospholipase A1-IIalpha (Q9LNC2.1), Phospholipase A1-IIbeta (O82274.2), Phospholipase A1-IIgamma (O49523.1), Phospholipase A1-IIdelta (Q9SJI7.1), DAD1-like acylhydrolase (Q9C8G6)] in the NCBI BLASTp using as database Reference proteins (refseq_protein) or Non-redundant protein sequences (nr). For each protein, serial blasts were performed in different organisms. The cutoff amino acid identity was 42 % with 55 % positives and E-values 5e-126 in order to be included in this analysis. The Triacylglycerol lipase of *Rhizomucor mieher* was used as outgroup, as it is known that it contains the conserved sequence characteristics (catalytic triad and GXSXG motif) and its protein structure has been analyzed by X-ray crystallography [8,45]. The representatives from Angiosperms were collected by scanning all plant groups based on the APG IV system focused on rosids. From Basal Angiosperms, *Amborella trichopoda* was selected and from Monocots, *Asparagus officinalis*, *Oryza*

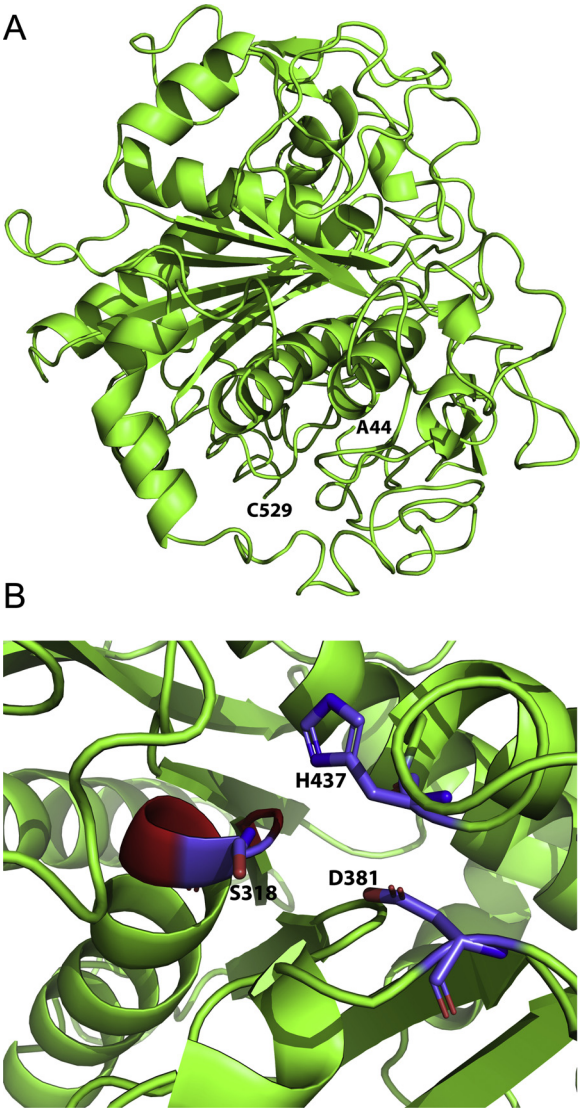

Fig. 2. Modeling of AtDALL3. (A) A cartoon representation of AtDALL3 structural model (colored in green), displayed using the software PyMOL. The overall structure of AtDALL3 is comprised of a central beta sheet surrounded by a-helices. (B) The catalytic triad, which is conserved among lipases, is also present in AtDALL3. It is formed by residues Ser318, Asp381 and H437. The catalytic residues are represented as stick models. The G-X-S-X-G consensus sequence (residues 316–320) containing the catalytic serine is colored red. (For interpretation of the references to colour in this figure legend, the reader is referred to the web version of this article.)

sativa and *Zea mays*. The representatives from the eudicot clade were collected from the orders *Fabales, Malpigphiales, Fagales, Rosales, Myrtales, Sapindales, Brassicales, Malvales, Caryophyllales, Solanales, Asterales,* and *Proteales*. Furthermore, *Physcomitrella patens* was used as a member of Bryophytes while *Selaginella moellendorffi* of Lycopods.

All protein sequences were aligned with Clustal Omega (EMBL-EBI). The alignment was transferred to the program PAUP 4.0 beta Win [46], in order to construct Neighbour Joining and Maximum Parsimony trees. To run MrBayes, the best model was found (WAG + I + G + F) using PartitionFinder2 [47–49]. MrBayes v3.2.6 [50] was employed in order to run four independent MCMCMC searches using different random starting points and 1 M generations were applied with sampling every 5 K generations. Convergence was estimated with the PSRF index (Potential Scale Reduction Factor) [51] as it approached 1 and also checked visually by plotting likelihood scores vs. generation for the different runs. Based on this analysis, the burn-in was set to 25 %. The nodes from all three trees were compared using TreeGraph 2 (2.14.0-771 beta) [52]. Finally, reliability of nodes was assessed using 1000 and 100 bootstrap iterations for the NJ and MP, respectively, and posterior probabilities for the BI analysis. The BI tree is presented using FigTree v1.4.3 (http://tree.bio.ed.ac.uk/software/figtree/).

2.11. Protein molecular modeling

A three dimensional (3D) model of Phospholipase PLA1-Iγ2 or otherwise DAD1-LIKE LIPASE 3 (DALL3) from *Arabidopsis thaliana* was predicted by using I-TASSER (Iterative Threading ASSEmbly Refinement), an online server for automated protein 3D structure and function prediction from protein primary structure (https://zhanglab.ccmb.med.umich.edu/ITASSER) [53,54]. During the procedure, we applied the default parameters of the software. The amino acid sequence of DALL3 from *Arabidopsis thaliana* was retrieved from Uniprot [55] (Accession number Q3EBR6) and consists of 529 residues. Residues 1–43 correspond to the transit peptide that is responsible for the transport of the protein to the chloroplast.

Our attempt to build a structural model of DALL3 involved the mature form of the protein (residues 44–529) that is located in the chloroplast. The structural model of DALL3 was constructed from multiple threading alignments and iterative structural assembly simulations. Comparison of the produced models with other known protein structures provides insights for the function of proteins being investigated [56]. The derived model was subsequently subjected to energy minimization utilizing GROMACS v. 2016.3 [57] and the AMBER 99SB-ILDN force field [58] in order to remove clashes between side chains. Images containing structural models were generated through the PyMol Molecular Visualization System (http://www.pymol.org).

3. Results and discussion

3.1. Sequence characteristics of AtDALL3 and 3D modeling

To study the function of SBP in plants we screened an Arabidopsis cDNA library for potential interacting proteins of SBP1 using the yeast two-hybrid system. Amongst the clones we identified in this manner was the chloroplastic/plastidial Phospholipase A1-Igamma2 (AtDALL3) [24]. AtDALL3 (Q3EBR6, At2g30550) constitutes a protein of 529 aa (Fig. 1A). It contains a conserved domain between amino acids 316–320 defined by the sequence GXSXG and a catalytic triad which is constituted by serine (aa318), aspartic acid (aa381) and histidine (aa437) residues (Fig. 1B).

AtDALL3 is a member of the alpha/beta hydrolase superfamily. This superfamily has the most widespread protein fold [59] in all domains of life with different catalytic roles in metabolism, comprising esterases, thioesterases lipases, proteases, dehalogenases, haloperoxidases and epoxide hydrolases [59–62]. These proteins share a highly conserved three dimensional architecture, although the sequence identity is very low [60].

The first lipase structures of triacylglycerol lipase [45] were determined by X-ray crystallography in *Rhizomucor miehei* and in human pancreas [63]. Lipases, except the characterized fold, share a conserved catalytic triad and possess the consensus motif GXSXG. More specifically, the core fold is an 8-stranded β-sheet with only the second strand antiparallel (β2) and the β3-β8 strands connected by α-helices. The three dimensional architecture reveals that the active site is surrounded by three loops β5, β9 and a lid domain [64]. The lid domain is composed of one or more α-helices, joined to the main structure of the enzyme by a flexible structure. It is a mobile element which uncovers the active site under the appropriate conditions [18,65–68]. Moreover, lipases are characterized by disulfide bridges that are important for enzyme stability and catalytic activity [18].

The conserved catalytic triad consists of a serine as nucleophile residue, an aspartate/glutamate as the acidic residue and a histidine

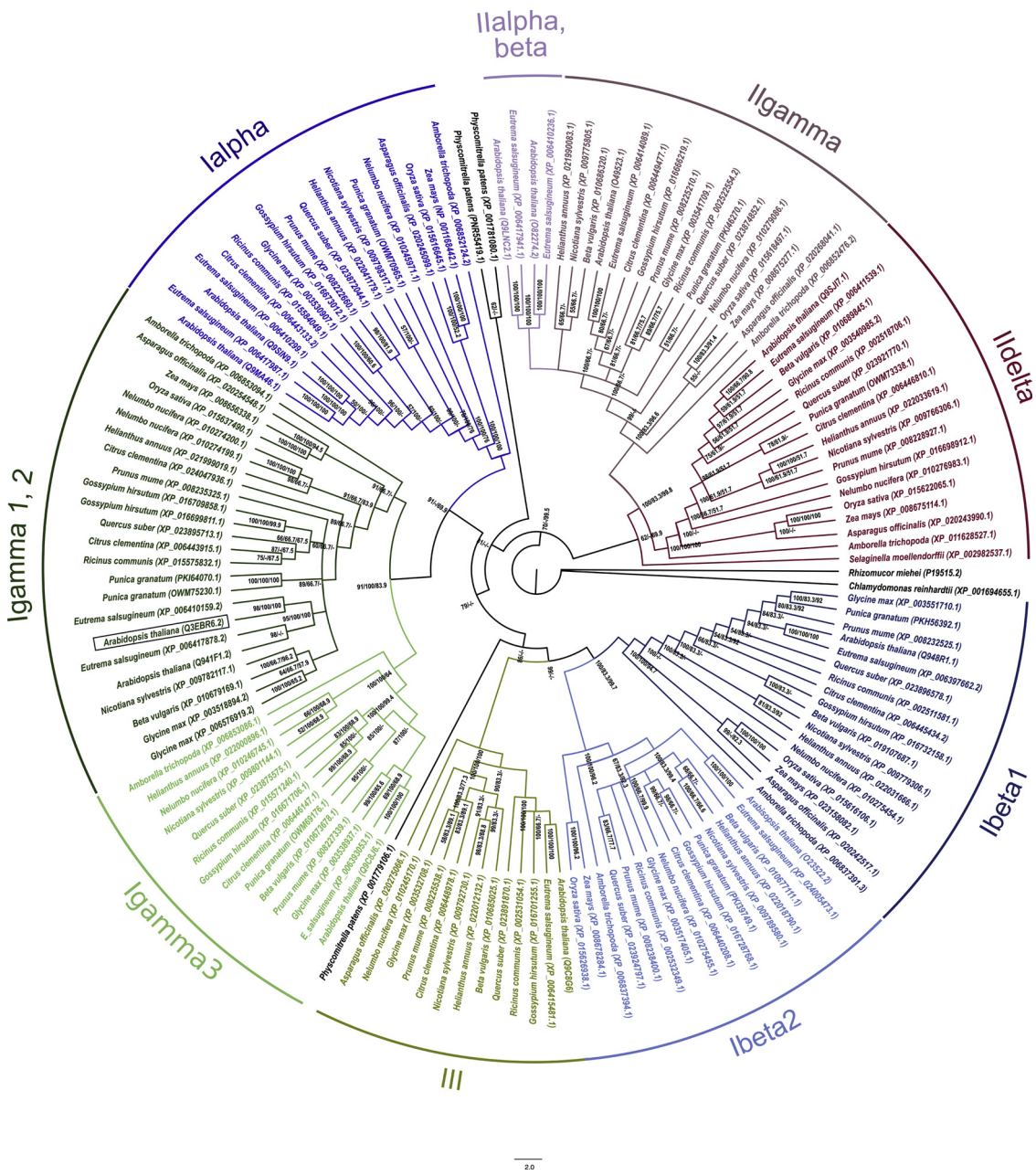

Fig. 3. Phylogenetic tree of the DAD1-Like Lipases Family in Angiospermae. Phylogenetic tree constructed by the amino acid matrix of phospholipases as produced by Bayesian (BI) analysis. The phosholipase of *Chlamydomonas reinhardtii* was used to root the tree. Clade credibility using PP (1st number), MP and NJ-bootstrap (2nd and 3rd number, respectively) are shown. The different coloring used as follows, blue: PLA1-Ibeta1, light blue: PLA1-Ibeta2, brown: PLA1-III, light green: PLA1-Igamma3, green: PLA1-Igamma1,2, electric blue: PLA1-Ialpha, light mauve: PLA1-IIalpha,beta, mauve: PLA1-IIgamma, red: PLA1-IIdelta. The phospholipases are divided based on the *At*DAD1 family classification. The formed clades are grouped based on the presence of each protein in *At*PLA1-Ialpha, *At*PLA1-Ibeta1, *At*PLA1-Ibeta2, *At*PLA1-Igamma1, 2, *At*PLA1-Igamma3, *At*PLA1-IIalpha, beta, *At*PLA1-IIgamma, *At*PLA1-IIdelta and class III. *At*DALL3 (*At*PLA1-Igamma2) is boxed. (For interpretation of the references to colour in this figure legend, the reader is referred to the web version of this article.)

[45,60,63]. The catalytic serine is located after the β5 strand and before the following α-helix. The acidic residue (Asp/Asn) is almost always positioned after strand β7 and the histidine residue located in the loop after the last β strand [18,59,69]. Carriere et al. [64], showed that the difference between animal phospholipases A1 and lipases is based on the shorter β9 loop and lid domain of PLA1, features that increase the active site accessibility.

Since there is not an experimentally determined 3D structure of DALL3 from *Arabidopsis thaliana* a theoretical model was built by I-TASSER server, providing as input the sequence of DALL3 from Uniprot, excluding the transit peptide (residues 1–43). Estimation of the quality of the predicted model by I-TASSER was done by calculation of the C-score, the template modeling score (TM-score) and the root mean square difference (RMSD). C-score is a confidence score that its value typically ranges from -5 to +2. A high value of C-score indicates high confidence of the model. TM-score is a scale for measuring the structural similarity between two proteins with different tertiary structures. A value of TM-score over +0.5 indicates that the topology of the predicted model is correct, while a value below +0.17 indicates random similarity. In this case, the values of C-score, TM-score and RMSD in correlation with the C-score for the predicted model are -1.16, 0.57 ± 0.15 and 9.9 ± 4.4 Å, respectively. These values indicate that our predicted model is reliable and that can be used for analysis and suggestion of the structural features of DALL3 from *Arabidopsis thaliana*.

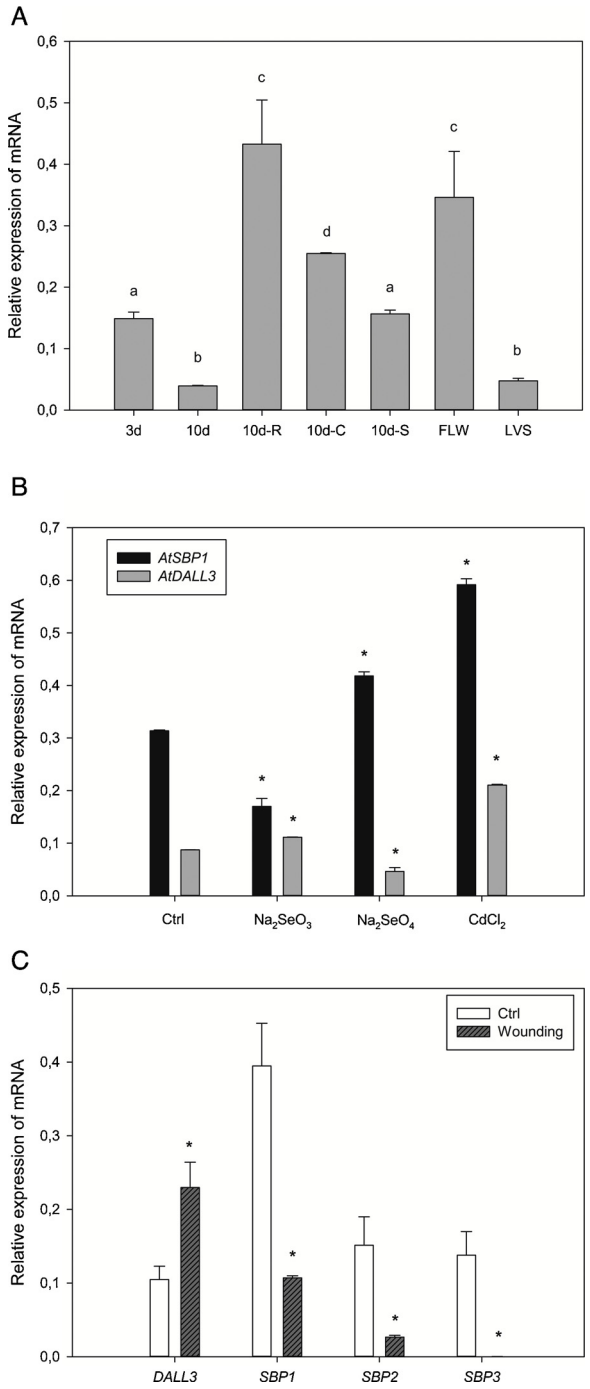

Fig. 4. Gene expression analysis of *At*SBP1 and *At*DALL3. (A) Relative expression of *AtDALL3* in *Arabidopsis thaliana* tissues at different developmental stages. 3d: 3 days old seedlings, 10d: 10 days old seedlings, R: Root, C: Cotyledons, S: Shoots, Flw: Flowers and Lvs: Rosette leaves. (B) Relative expression of *AtSBP1* and *AtDALL3* in *Arabidopsis thaliana* in plants treated with selenium and cadmium compounds. There is significant upregulation of *SBP1* and *DALL3* genes upon treatment with cadmium. (C) Relative expression of *AtSBP1* and *AtDALL3* in *Arabidopsis thaliana* in response to wounding. Two-fold induction of *AtDALL3* is observed in relation to significant downregulation of *SBP* genes.

In all three experiments values ± SD were normalized to the geometrical mean of *UBQ10* and *PP2A* and represent the mean of three biological samples analyzed in triplicate. Significant differences at $P \leq 0.05$ are indicated by different letters (A) and asterisks (B, C).

The model was further subjected to energy minimization utilizing GROMACS in order to refine its geometry and remove clashes between side chains.

Observation of the structure shows that it is composed of a central parallel β-sheet, with the second strand antiparallel, surrounded by α-helices (Fig. 2A). These findings indicate that DALL3 belongs to the class of α/β proteins adopting the alpha/beta-hydrolase fold that is present in lipases [18]. This conclusion is supported by the results retrieved, when our model was scanned against the classified domains in CATH database [70], a publicly-accessible, online resource of protein domain structure classification of experimentally determined 3D structures deposited in Protein Data Bank (PDB) [71]. The similarity of the domains from CATH with the submitted structure is calculated by the Sequential Structure Alignment Program (SSAP) method [72]. In general, SSAP scores above 80 are associated with highly similar structures. All the structures (PDB codes 2YIJ, 3 TG L and 1UWC) that match best to the model of DALL3 (with values of SSAP score > 80) are classified as ab proteins at the Class level, forming a 3-Layer (aba) Sandwich at the level of Architecture. Besides the SSAP score, the RMSD value between the model and the structure that was used as template for model construction (PDB ID 2YIJ) is 0.8 Å, indicating high similarity between the two structures. Furthermore, an additional research regarding these PDB entries in SCOPe database [73] indicated that they belong to the Class of α/β proteins that adopt alpha/beta-hydrolase fold, further supporting our suggestion that DALL3 adopts this fold. As far as the catalytic residues of DALL3 are concerned, the conserved domain between amino acids 316–320, defined by the sequence GXSXG, and a catalytic triad, constituted by serine (aa318), aspartic acid (aa381) and histidine (aa437) residues, are in close proximity in the proposed model, allowing this way to perform its catalytic role (Fig. 2B).

3.2. Phylogenetic analysis of AtDALL3

Phylogenetic analysis of DALL3 was performed in order to examine if its amino acid sequence coincides with the expected data of all PLA-Igamma2 lipases. Moreover, in this work there was an effort to classify all different lipases from representative plant species of Angiosperms (Supplementary table 1). Our analysis showed that DALL3 appears in the PLA1-Igamma1 as expected, which groups with PLA1-Igammma2 OTUs (Fig. 3).

The DAD1-like lipase family is divided into three classes, based on the presence of N-terminal stretches and sequence similarities in the catalytic region. Class I consists of chloroplastic proteins, class II of four cytoplasmic proteins, while class III of one mitochondrial isoform [8]. In the phylogenetic tree (Fig. 3), it is evident that the class II is completely divided from the other classes and is further divided into four clusters: PLA1-IIalpha, PLA1-IIbeta, PLA1-IIgamma and PLA1-IIdelta. PLA1-IIalpha and PLA1-IIbeta that are present only in *Arabidopsis thaliana* and *Eutrema salsugineum* (most probably only in the Order *Brassicales*) are fully supported (i.e., PP, MP, NJ bootstrap 100 %). PLA1-IIgamma and PLA1-IIdelta lipases clustered well, containing all representatives of each enzyme category with excellent support (100/ 83,3/ 96,6 % and 100 %, respectively) no matter the bootstrap method used. Moreover, these two groups clustered as sister clades with perfect support (i.e. 100/ 83,3/ 99,8 %). The sole exception was the lipase of *Selaginella moellendorffii* which was placed outside the IIgamma and IIdelta lipases. This may be due to the unique representation of the lipase's gene in the genome of this species (data not shown). Additionally, Selaginella is evolutionary suggested as a living descendant of the land vascular plant ancestor [74,75], which may further verify its unique topology.

Moreover, the chloroplastic proteins of PLA1-Ibeta1, which are renamed as DAD1 proteins (DEFECTIVE ANTHER DEHISCENCE 1) [8,20], and those of PLA1-Ibeta2 are clustered as sister clades with outstanding support (100/ 83,3/ 99,7 %) (Fig. 3). All examined species

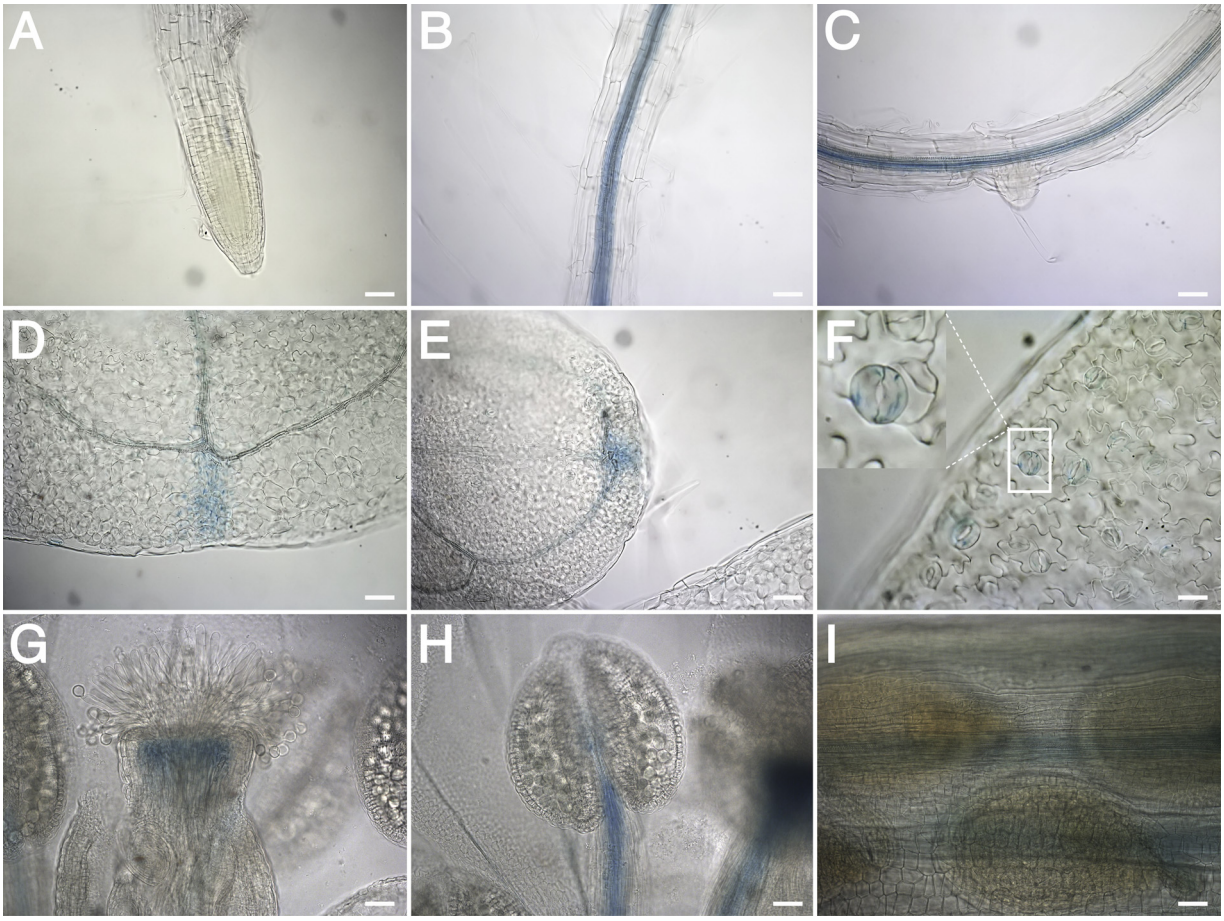

Fig. 5. Analysis of *At*DALL3 promoter activity in *Arabidopsis thaliana* plants transformed with GUS gene reporter fusions. GUS expression is observed in the hydathodes, the guard cells of cotyledons and first leaves (D–F) and the vasculature of all examined tissues. A-C: Root, D: cotyledons, E: First leaves, F: Guard cells of cotyledons, G: Stigma, H: Filaments, I: Siliques. Bars 50 μm. (For interpretation of the references to colour in this figure legend, the reader is referred to the web version of this article.)

contained both isoforms of PLA1-Ibeta with the exception of *Asparagus officinalis* and *Physcomitrella patens*. The first species lacked the Ibeta2 isoform and the second species had no such protein.

The isoforms PLA1-Ialpha1 and PLA1-Ialpha2 are both present in *Arabidopsis thaliana* and *Eutrema salsugineum*, while the other species contain one of the isoforms. For the PLA1-Igamma1, 2 and 3, most of the studied species contain all three isoforms except the representatives of the order Poales that contain only the PLA1-Igamma1, while in *Beta vulgaris* and *Amborella trichopoda,* PLA1-Igamma2 is absent (Supplementary Table 2). The PLA1-Igamma3 is basal to the other two isoform categories with very good support (91/ 100/ 83,9 %).

The only protein that is characterized as mitochondrial is that of the *Arabidopsis thaliana* [8,76]. In the constructed phylogenetic tree, the clade that includes this protein is grouped with proteins which were previously characterized as PLA1-Igamma1 but in our analysis they excised from the respective PLA1-Igamma1 group that clusters with PLA1-Igamma2 (Fig. 3). However, most of the proteins are characterized as predicted. Furthermore, this group is rather closely related to the isoforms PLA1-Ibeta1 and beta2, than the PLA1-Igamma, introducing the notion of an organellar close relationship.

This phylogenetic analysis shows that the class II might be the ancestor of the other chloroplastic and mitochondrial DAD1-like lipases where PLA1-IIalpha and PLA1-IIbeta appears only in Brassicales, and thus, this may be a late evolutionary event. PLA1-Igamma proteins seem to be relatives of PLA1-Ialpha. However, there are different PLA1-Igamma isoforms which are closely related to PLA1-Ibeta and group with the mitochondrial PLA1. Considering the fact that these proteins are characterized as putative then it might be possible that they are misannotated due to the lack of experimental evidence. Thus, it may be suggested that they are of mitochondrial origin, since the mt PLA1 is fully and well characterized in *Arabidopsis thaliana* [76].

3.3. Gene expression analysis of AtDALL3 during development and abiotic stress

Initially, we studied the relative expression levels of *AtDALL3* mRNA in developing tissues of *Arabidopsis thaliana* (Fig. 4A). The highest level of expression was observed in 10-day-old roots and in flowers, while constitutive levels were maintained in seedlings, cotyledons, shoots and leaves. A three-fold downregulation of DALL3 occurred in 10-day-old seedlings when compared to earlier stages of development (3-day-old seedlings). RT-PCR experiments from Seo et al. [16] who studied the expression of the seven Class I chloroplastic proteins, have shown the constitutive expression of DALL3 being elevated in 4d-seedlings, stems and rosette leaves. Comparison of our data with those of GENEVESTIGATOR shows evidence that in the bolting stage expression in rosette leaves decreases.

Regulation of *DALL3* expression under abiotic stress conditions has previously been reported [22]. Furthermore, we have recently shown that AtSBP1 (an interacting partner of AtDALL3) is diff ;erentially regulated at the gene expression level by sodium selenite (Na_2SeO_3) and sodium selenate (Na_2SeO_4) [34] and is upregulated by cadmium ($CdCl_2$) [77,78]. Thus, it would be interesting to determine the relative transcript accumulation of *AtDALL3* after treatment of plants with the

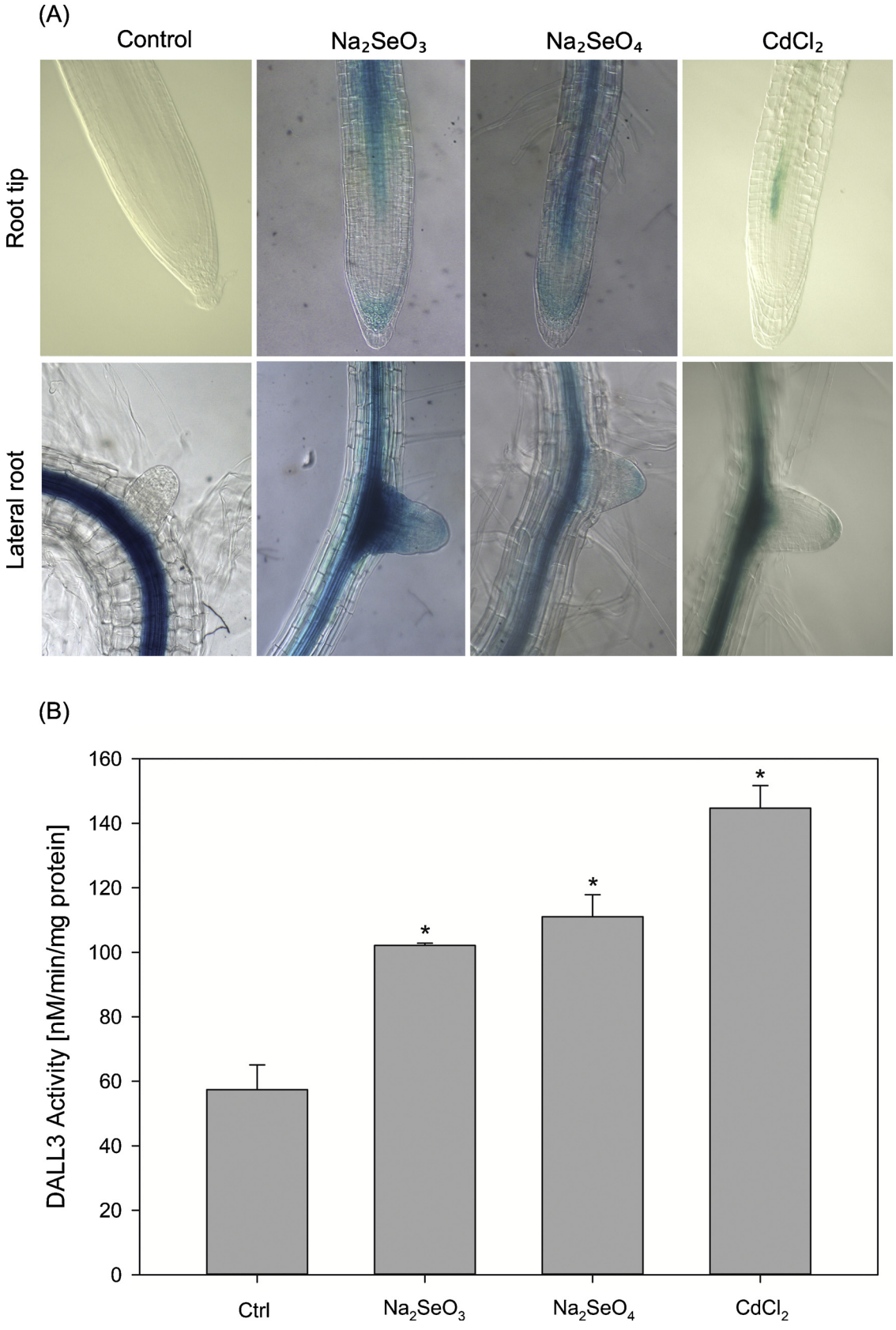

Fig. 6. Responses of *At*DALL3 promoter to abiotic stress. (A) Histochemical GUS assays defining the response of *DALL3* promoter to selenium and cadmium compounds as observed in the root apex and lateral root primordia. *At*DALL3 promoter differentially regulates GUS expression in distinct cell files depending on the compound used. (B) GUS activity in Arabidopsis plants transformed with *At*DALL3 promoter construct under physiological conditions and after treatment with selenium and cadmium compounds. Fluorometric GUS assays were performed in triplicate and the mean value was calculated. Error bars represent SD. Significant differences at $P \leq 0.05$ are indicated by asterisks. Specific GUS activity is shown in units of nanomoles 4-MU produced per milligram of protein per minute. All measurements were repeated three times on eight to 12 independently transformed plants. (For interpretation of the references to colour in this figure legend, the reader is referred to the web version of this article.)

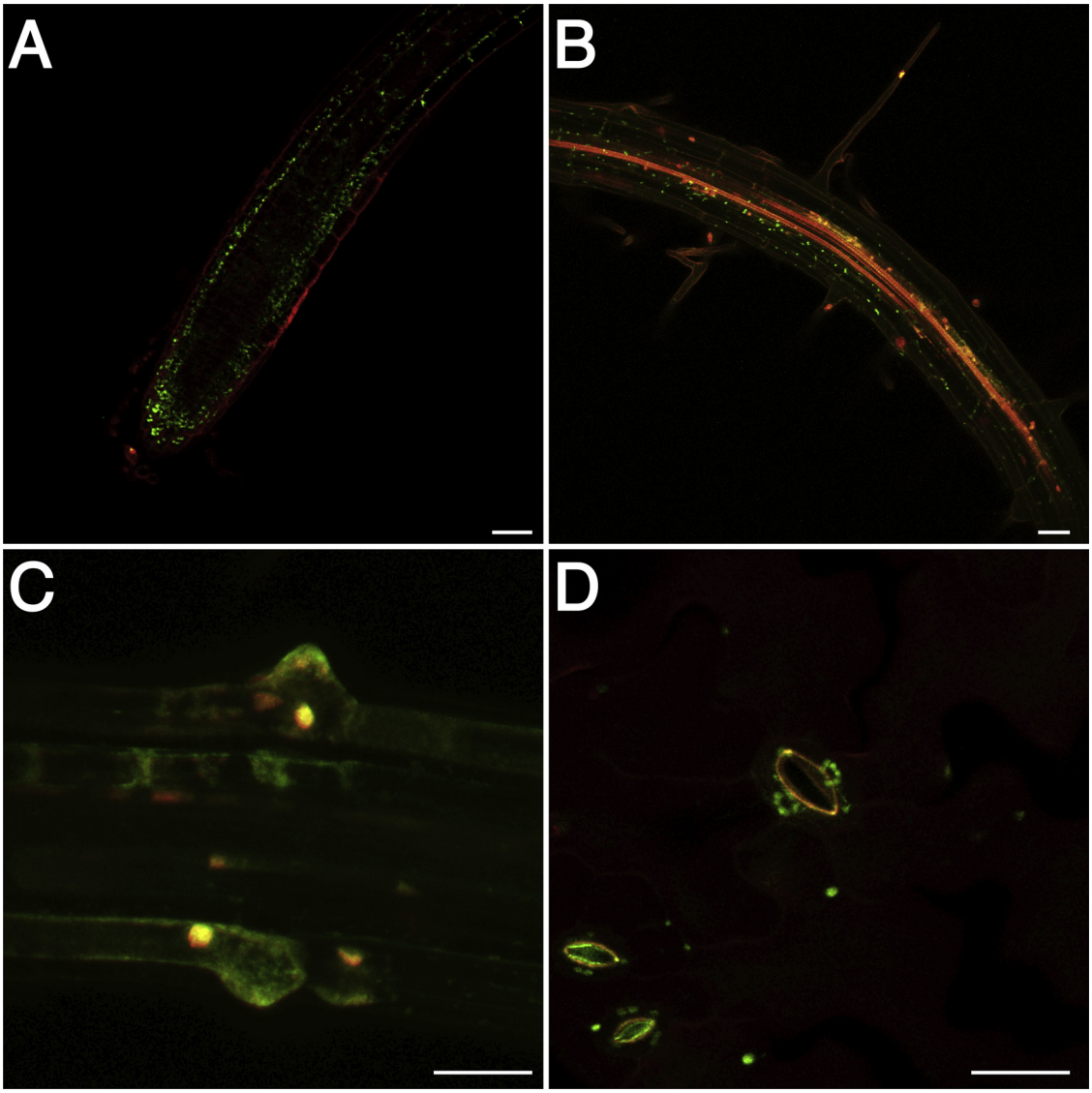

Fig. 7. Sub-cellular localization of *At*DALL3 in 10 days old seedlings of chimeric *At*DALL3::eGPF stably transformed plants. Confocal microscopy reveals GFP signal in the plastids of the root apex (A) and endodermis along the root stele (B), in the cytoplasm of lateral roots (C) and in chloroplasts of guard cells of the stomata (D). Bars 34 μm. (For interpretation of the references to colour in this figure legend, the reader is referred to the web version of this article.)

aforementioned compounds. Therefore, we investigated the gene expression patterns of the *AtSBP1* and *AtDALL3* in control plants, as well as, in response to treatments with cadmium and selenium compounds (Fig. 4B). Our analysis showed that *AtDALL3* is marginally upregulated by 150 μM Na_2SeO_3 and significantly downregulated by 150 μM Na_2SeO_4. A statistically notable, concerted induction of *AtSBP1* and *AtDALL3* was recorded in response to 150 μM $CdCl_2$. Overall, our data further strengthen previous observations that indeed *AtSBP1* gene is diff ;erentially regulated by cadmium, selenite and selenate [34,77,78], but we show additionally that also *AtDALL3* participates in the network of genes regulated in response to these compounds.

In *Arabidopsis thaliana*, it has been shown that, oxidative stress due to cadmium exposure relates to hydrogen peroxide accumulation [79] and that treatment of plants with selenium compounds led to ROS accumulation in the roots [34]. It has also been proposed, that in addition to the importance of SBP1 in stress responses, SBP1, may be part of a protein network that responds to the cellular redox state [34].

Heavy metals cause modifications in the lipid cellular component [80], a process depended on phospholipase activity. Furthermore, cadmium and ROS can lead to the mobilization of proteins including phospholipases C and D, producing secondary messenger molecules [81,82]. Interestingly, there are many studies connecting the oxidative stress caused from Cd and heavy metals with the increasing production of Jasmonic acid [83–87], probably affecting growth procedures [87]. Taking into account our data, the JA upregulation could be due to DALL3 and other DAD1-like lipases, which participate in JA biosynthesis.

There are many studies connecting DALLs with wounding and JA biosynthesis. It is known that JA is induced by wounding and pathogens. Microarray studies showed that there are no significant changes in the transcription levels 30 min after wounding [22], while Ruduś et al. [20] revealed a significant increase in the relative expression 80 min after wounding. Furthermore, JA levels halved in the DALL3 knockout [21]. The mechanism by which DALL3 participates in wound induction, is still not clear, but evidence shows that this occurs in a COI1- and JA-independent manner [20].

Consequently, we investigated how wounding influences the regulation of SBP gene family in comparison to DALL3 (Fig. 4C). Wounded plants were assayed for gene expression of *AtDALL3*, *AtSBP1*, *AtSBP2* and *AtSBP3* over control plants. As expected, *AtDALL3* demonstrated a 2,5-fold induction upon wounding, a response which is in line with previous studies [20]. Interestingly, a significant decrease of the

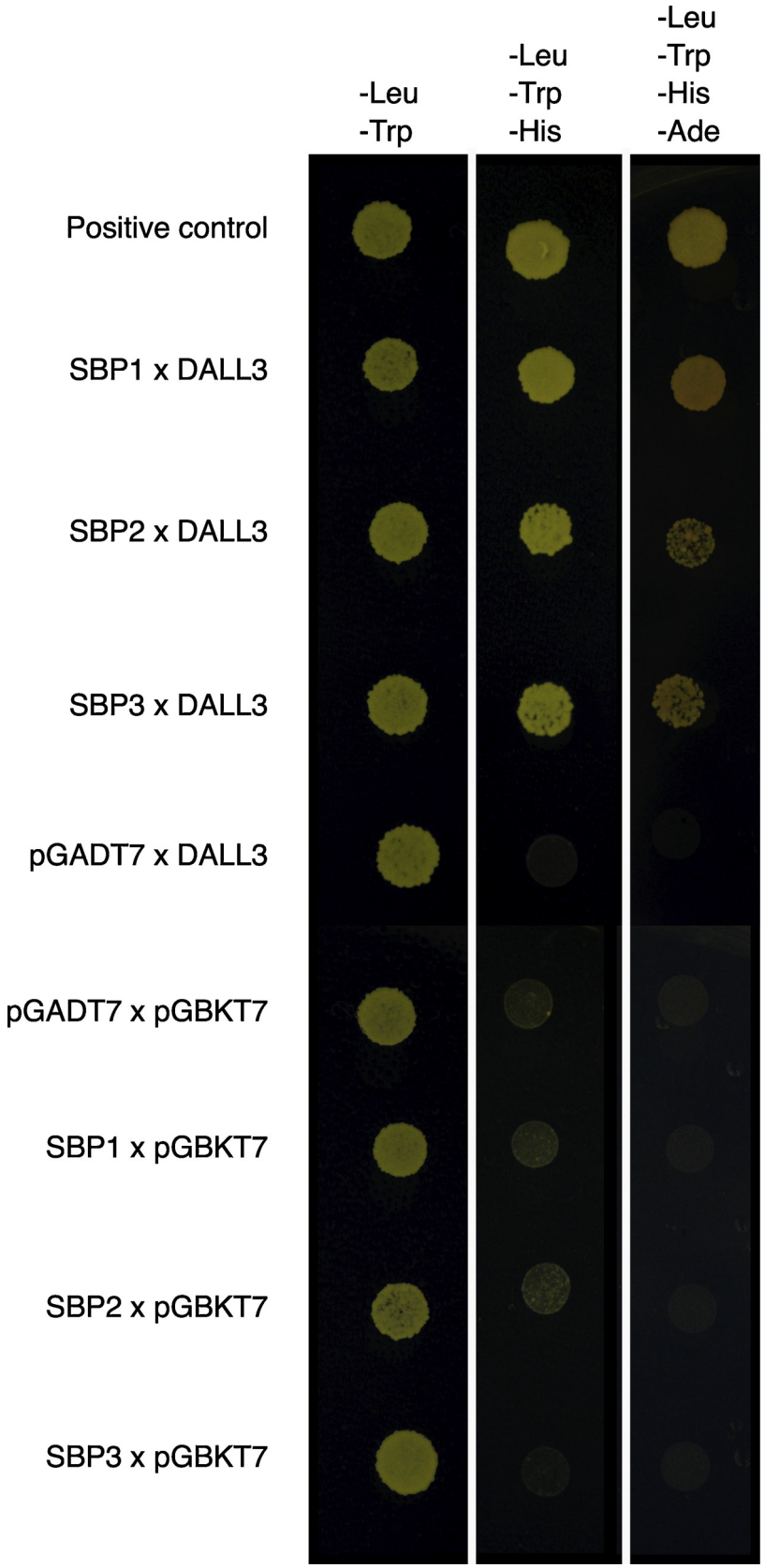

Fig. 8. Yeast two-hybrid assay. *in vivo* interaction of *At*DALL3 with all members of the *At*SBP protein family in yeast. Proper controls to exclude unspecific vector activation were included along with the 53/T positive control.

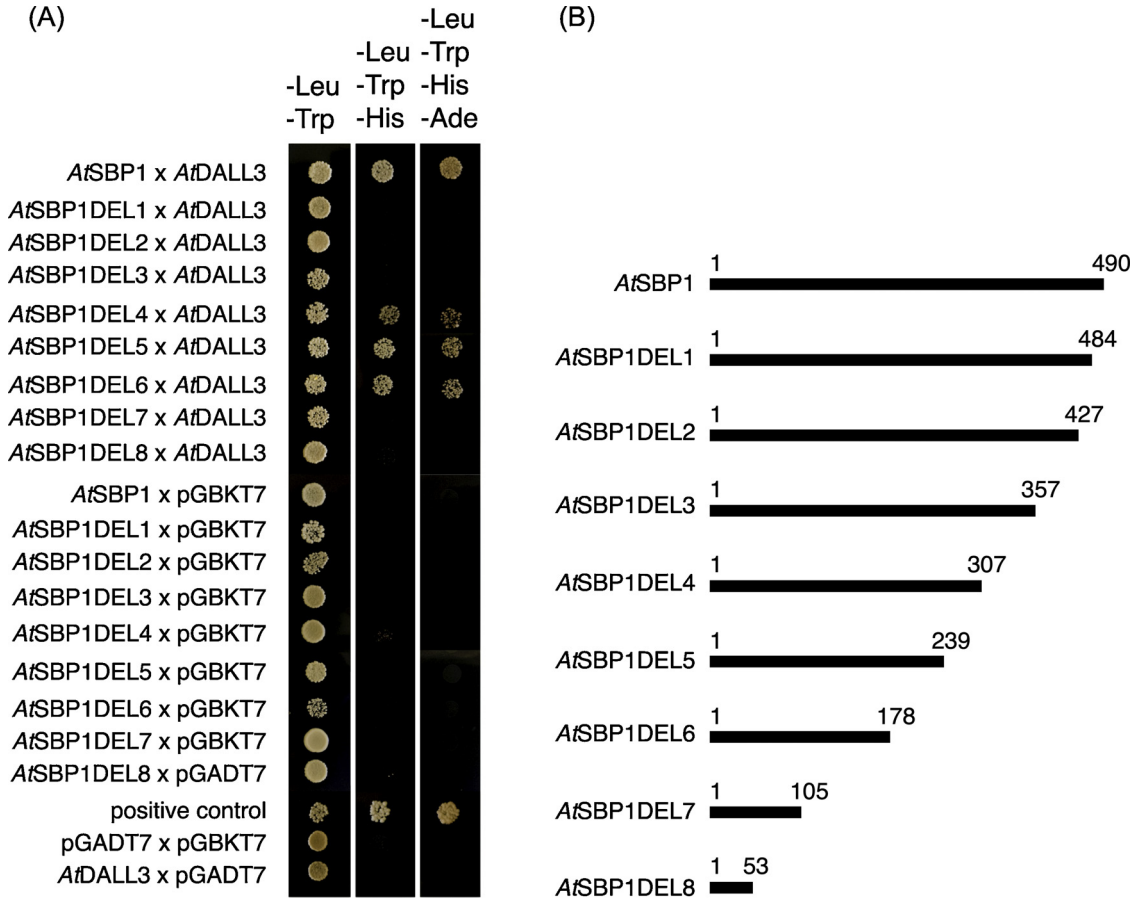

Fig. 9. Physical interaction of *At*DALL3 as revealed by deletion analysis of *At*SBP1. (A) The shortest truncated version of *At*SBP1 that interacts with *At*DALL3 is *At*SBP1DEL6 of 178 N- terminus amino acids. (B) The truncated polypeptides of *At*SBP1 used for deletion analysis in (A). Several negative controls to exclude unspecific activation were included.

expression levels of all the members of the *SBP* gene family was observed. A rapid increase in H_2O_2 level, commonly known as an oxidative burst, occurs in plant tissue after wounding [88,89]. Our previous results have provided evidence that at least SBP1 expression is tightly linked to detoxification processes related to oxidative stress, since it is downregulated in ROS-induced plants in the presence of N-acetylcysteine [34], a thiol-containing antioxidant of low molecular weight with free-radical-scavenging properties [90,91]. Examples of downregulated stress sensors, though, there exist. Swindell has shown [92], that in nine abiotic stress treatments (including wounding) the auxin-responsive (At3g20220) and the auxin-regulated (At2g21210) chloroplast proteins were both downregulated. The downregulation of auxin-responsive genes had been previously documented as a response to wounding stress, but such downregulation had not previously been noted under other abiotic stress treatments [93]. Thus, it is tempting to speculate that at least in response to wounding, downregulation of SBP genes may be considered part of a stress signaling mechanism.

3.4. Promoter activity of AtDALL3

To investigate the transcriptional potential of the *DALL3* promoter in Arabidopsis, we generated transgenic plants harboring a 622 bp fragment, located upstream the transcriptional start site, fused to the *GUS* reporter gene (pr*DALL3::GUS*). This 622 bp fragment was chosen after promoter deletion analysis of a 2804 bp fragment (data not shown). The analysis of the reporter gene activity in the roots and the aerial parts of the plants in independent transgenic lines revealed a spatial expression pattern of the *DALL3* gene (Fig. 5). *GUS* expression was detected neither in the root apex, the meristematic and elongation zones (Fig. 5A), nor in protruding lateral root primordia (Fig. 5C). In the root tissues examined, GUS staining primarily localized in the vascular cylinder of the main root (Fig. 5B, C) with a more intense signal in the xylem (Fig. 5B). In the aerial parts of the plant GUS staining was observed in the hydathodes and the vasculature of cotyledons and of the first emerging leaves (Fig. 5D, E), as well as, in the stomata (Fig. 5F). Furthermore, in the reproductive organs, GUS signal was detected in the stigma (Fig. 5G) and the vascular tissue of the stamen and the ovaries (Fig. 5H, I).

The expression patterns revealed with the above approach were overlapping with the patterns reported for *AtSBP1* gene [34] indicating that *DALL3* and *SBP1* transcripts co-localize. Hydathodes enable water conduction [94] and are the primary sites of the high-level production of free auxin in developing leaf primordial [95]. In corn, there is *in vivo* evidence that phospholipase A is involved in the signal transduction pathway of auxin induced coleoptile elongation [96]. It was proposed that phospholipase A is activated by auxin and that the products of the enzyme, lysophospholipids and fatty acids, induce acidification of the apoplast by activating the H^+-pump [96].

It is known that hormones cooperate in different ways and are implicated in several processes. Auxin and jasmonic acid can work synergistically or antagonistically upon systemic functions. There are studies indicating that some phospholipases A are induced by auxin [97,98] whereas the fatty acids and lysophospholipids produced by pospholipases act as potential second messengers in auxin action [98]. Generally, it is proposed that phospholipases A play an important role in the regulation of auxin responses [99]. It has also been shown that genes associated with auxin and jasmonic acid cooperate to form a functional, fertile anther [100]. Specifically, in Arabidopsis anther

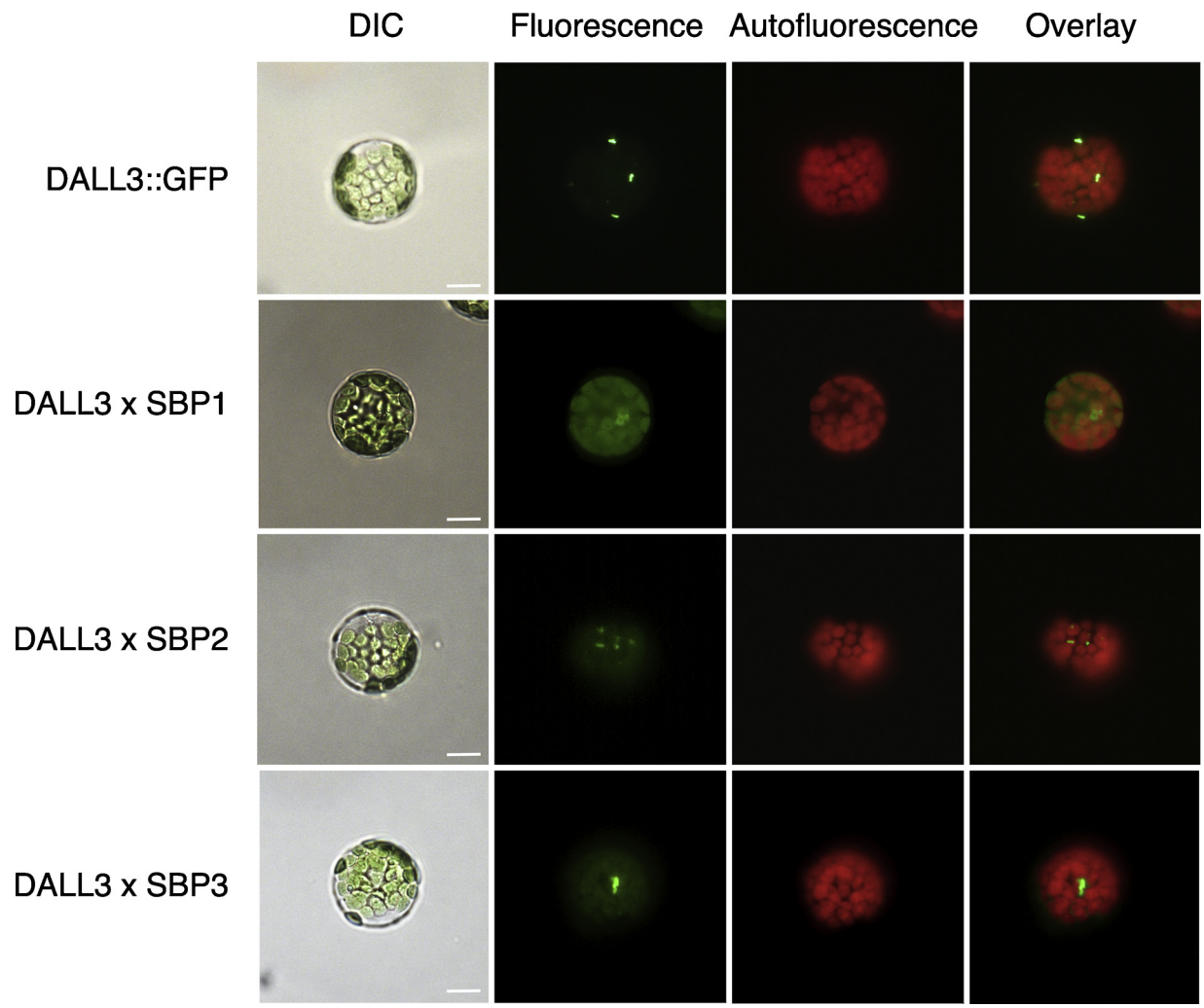

Fig. 10. Transient expression of *At*DALL3 and BiFC assays in Arabidopsis protoplasts. *At*DALL3 was fused to GFP and nCerulean to generate chimeric constructs while SBPs were fused to cCFP. *At*DALL3 interacts *in planta* with all *At*SBPs in speckle-like structures in the chloroplast's surface, where *AtDALL3* is detected too. Bars 25 μm. (For interpretation of the references to colour in this figure legend, the reader is referred to the web version of this article.)

development is a process controlled by auxin, which regulates ARF genes, via an unknown mechanism. ARF6 and ARF8 indirectly activate *DEFECTIVE IN ANTHER DEHISCENCE1* (*DAD1*), which is the first gene in JA biosynthesis [100–102].

We further studied the effect of selenium and cadmium compounds on DALL3 promoter activity. Fig. 6 summarizes the tissue specific expression changes and the fluorometric GUS activity in young chemically treated Arabidopsis plants. Major changes in GUS expression patterns were primarily observed in the root apex and the lateral roots of young seedlings (Fig. 6A). Sodium selenite and sodium selenate treatments induced GUS expression in the central cylinder and to some extent in the surrounding cortical cells. Staining was also evident in most collumella and lateral root cap cell layers, including the collumella initials. On the contrary, and in line with the untreated roots, *DALL3* is not expressed in the quiescent center and the cells of the meristematic zone. Additionally, while in untreated plants no GUS expression was observed in lateral root primordia strong induction in a tissue-specific manner was documented upon treatment with all the compounds tested (Fig. 6A). Staining was evident in the founder cells of the pericycle that initiate the formation of the lateral root primordia and the differentiating root cap cells. As with the primary root, *DALL3* expression was absent in the meristematic zone of the lateral roots. These observations are further validated by measuring GUS activity changes driven by the DALL3 promoter in intact young seedlings when treated with the aforementioned compounds (Fig. 6B). The highest overall induction of GUS activity was observed in treatments with cadmium chloride (2,5-fold change) when compared to the control untreated samples. Selenium compounds also elicited changes in activity indicating the differential response of DALL3 promoter. Both selenium compounds and cadmium chloride induce a two- to three-fold induction of gene expression compared to the control untreated samples, indicating the differential response of DALL3 promoter (Fig. 6B).

3.5. Localization of AtDALL3::EGFP fusion by confocal microscopy

To gain insight into the localization of DALL3 protein in Arabidopsis we generated stably transformed lines with the AtDALL3::EGFP translational fusion and assayed intact plants (Fig. 7). It was interesting to observe that tissues negative for GUS staining (e.g. root apex and lateral roots) (Fig. 5A, C), were positive for the chimeric protein expression (Fig. 7A, C). In more detail, GFP signal was detected in the plastids of the root apex (Fig. 7A), the plastids of the central root (Fig. 7B) and the apex of emerging lateral root primordia (Fig. 7C). This indicates that the mature DALL3 protein is transported to these cell types following gene expression in the particular aforementioned tissues. The only overlap between gene expression and protein localization observed, was in the stomata (Figs. 5F and 7 D). As shown in Fig. 7D, DALL3 localizes in the periphery of the guard cells (orange color due to overlap

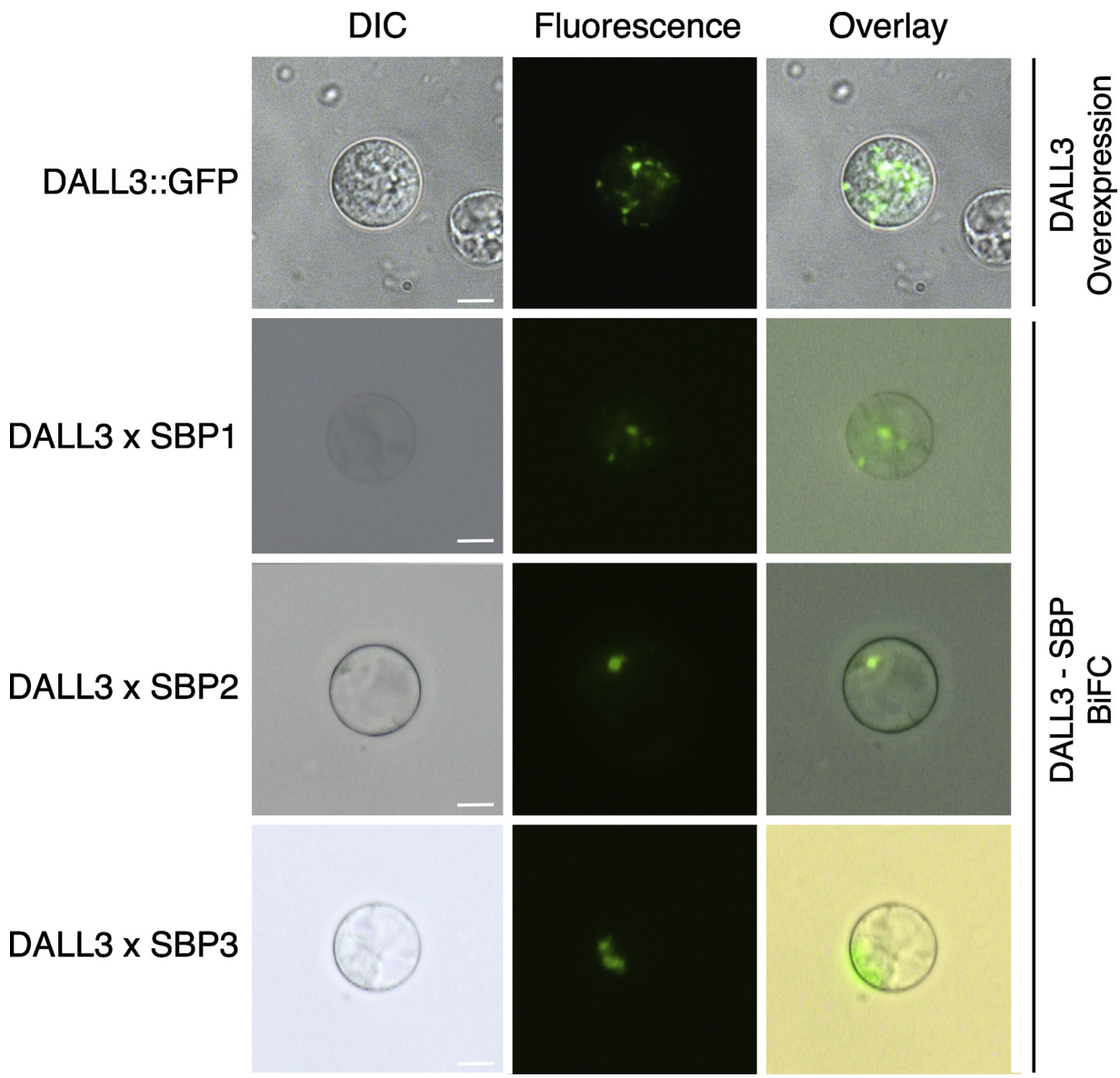

Fig. 11. BiFC assays in Arabidopsis root protoplasts. Isolated protoplasts from roots of 10 – days-old plants were transformed with DALL3::GFP and the interacting pairs of DALL3 and the SBP proteins of our BiFC system. The same plastidial localization pattern for the ectopically expressed DALL3 was observed and identical was the case for the interacting pairs of DALL3 with the three SBP proteins. Bars 15 μm. (For interpretation of the references to colour in this figure legend, the reader is referred to the web version of this article.)

of GFP and PI staining) and in the characteristic “donut” shape the chloroplasts form, around the nucleus of the guard cells. The available few studies on the localization of DALL3 are mainly performed by transient protoplast transformation. Their results, however, support ours as they indicate a chloroplastic localization [16,103].

3.6. Analysis of AtDALL3 interactions with yeast two-hybrid assays

The identification of protein-protein interactions comprises a pre-requisite towards understanding protein networks and functions, as proteins normally function in macromolecular complexes. Describing such interactions, although it may be of great interest, it can be challenging, since they may be transient, or may involve diff ;erent partners and overlapping binding sites [104].

In order to verify the positive interaction of AtDALL3 with AtSBP1 revealed by the yeast two-hybrid (Y2H) screening (with AtSBP1 as bait), the respective genes were amplified from total Arabidopsis root RNA, cloned in appropriate vectors and individual protein-protein interaction experiments were performed. Additionally, AtSBP2 and AtSBP3 were also amplified and cloned due to their high degree of homology with the bait protein.

Yeast cells coexpressing various construct combinations in pairs, were used to study protein-protein interactions (Fig. 8). This assay confirmed initially a strong positive interaction of AtDALL3 with AtSBP1. Interestingly, all three AtSBP proteins also strongly interacted with AtDALL3. No unspecific activation was detected when bait and prey proteins were used in combination with the respective empty vectors (pGBKT7 or pGADT7). Our data point to the existence of a novel protein-protein interaction network, consisting of the selenium binding protein family and the plastidial DALL3. Taking into account the properties and the suggested functions of the participating proteins, it is plausible to speculate that this network is part of the plant’s response to oxidative stress.

Moreover, we tried to determine domains in the AtSBP1 polypeptide, responsible for binding of AtDALL3. We generated a series of C-terminal truncated AtSBP1 polypeptides (Fig. 9B) and studied in yeast

cells their binding capacity to AtDALL3. Firstly, we investigated whether these truncated polypeptides cloned in frame with the binding domain of GAL4 react in an unspecific manner with the activation domain of the empty vector (Fig. 9A). We then analyzed the auxotrophy of yeast cells while harboring in pairs AtDALL3 and each of the eight truncated polypeptides of AtSBP1 (Fig. 9A). Our analysis showed that the first 178 aa of AtSBP1 maintain strong, full binding capacity to AtDALL3, while the region between aa 427–490, when deleted, interferes with proper binding. It is noteworthy, that aa 1–178 were recently identified as the interaction region with the stress related glutaredoxin AtGRXS14 [33].

3.7. BiFC assays of AtDALL3 with the AtSBP protein family

It has been reported previously that the human SBP1 localizes in the cytosol and the nucleus [105–107], while studies in plants demonstrated the expression of SBP in cytoplasmically dense cell types and membrane vesicles [108]. Furthermore, we have recently shown that in Arabidopsis protoplasts SBP::GFP protein fusions can be present both in the cytoplasm and the nucleus [33]. In order to elucidate in which cellular compartment DALL3 is localized, we initially performed transient expression assays in Arabidopsis protoplasts (Fig. 10). DALL3 was translationally fused to GFP and used to transform rosette leaf protoplasts. This analysis showed that DALL3 protein fusion was present in speckle-like structures that seemed attached to the chloroplasts (Fig. 10). The speckle-like structures attached to the chloroplasts in DALL3 localization studies have been previously observed in a heterologous system, via transient expression assays in tobacco, where DALL3 and DALL4 were studied as phospholipases induced in plant defense [103]. Moreover, these structures can be noticed in studies for other chloroplastic proteins of the DAD1-like family, such as DGL [7,21] and DAD1 [7].

We then asked if the interactions revealed by the yeast two-hybrid screening occur *in planta*. To answer this question, we employed bimolecular fluorescence complementation (BiFC) to probe the protein interactions in living protoplast cells [109,110]. Arabidopsis protoplasts were transiently transformed with constructs of the interacting pairs in the pSAT vector system [109,111]. As shown in Fig. 10, AtSBP1 interacts *in planta* with AtDALL3 in speckle-like structures and in the chloroplasts, while similar structures with confined BiFC signal were revealed for the DALL3 x SBP2 and DALL3 x SBP3 interactions. Our subcellular localization analyses define for the first time the compartmentalized expression pattern of the AtDALL3 in a homologous system (Fig. 10). Furthermore, we show that when ectopically expressed the bait and prey proteins defined by our H2Y screening, interact *in planta* in the plastids of isolated protoplasts. It remains unclear and worth further investigation under which conditions the described interactions occur *in vivo*.

We further investigated the aforementioned interactions in a homologous chloroplast-free system, that is, root protoplasts of *Arabidopsis thaliana*. We used the protocol of Bargmann and Birnbaum [44] to isolate protoplasts from roots of 10 – days-old plants and transformed them with DALL3::GFP and the interacting pairs of DALL3 and the SBP proteins of our BiFC system. With this analysis, the same plastidial localization pattern for the ectopically expressed DALL3 was observed and identical was the case for the interacting pairs of DALL3 with the three SBP proteins (Fig. 11).

Class I phospholipases of DAD1-Like Lipase Family have been described and shown to be chloroplastic proteins [16]. Our results agree with previous studies; however, we noticed the speckle-like structures. Suchlike structures have been described before for outer membrane proteins [112,113] and for proteins which are located in the space between the outer and inner membranes of the chloroplast envelope [113]. For further investigation, we run an online algorithm for subchloroplast localization prediction, the LNP-Chlo [114], that also revealed an envelope localization.

Declaration of Competing Interest

The authors declare that the research was conducted in the absence of any commercial or financial relationships that could be construed as a potential conflict of interest.

Acknowledgements

This research is co-financed by Greece and the European Union (European Social Fund- ESF) through the Operational Programme “Human Resources Development, Education and Lifelong Learning” in the context of the project “Strengthening Human Resources Research Potential via Doctorate Research” (MIS-5000432), implemented by the State Scholarships Foundation (IKY) (Irene Dervisi). We thank the laboratory of Prof. E. Flemetakis (Agricultural University of Athens, Greece) for technical assistance and Michael Zachariadis, National Center for Scientific Research “Demokritos”, Institute of Biosciences and Applications for confocal assistance.

Appendix A. Supplementary data

Supplementary material related to this article can be found, in the online version, at doi:https://doi.org/10.1016/j.plantsci.2019.110357.

References

[1] G. Chen, C.L. Snyder, M.S. Greer, R.J. Weselake, Biology and biochemistry of plant phospholipases, CRC Crit. Rev. Plant Sci. 30 (2011) 239–258.
[2] X. Wang, Plant phospholipases, Annu. Rev. Plant Physiol. Plant Mol. Biol. 52 (2001) 211–231.
[3] S.B. Ryu, Phospholipid-derived signaling mediated by phospholipase A in plants, Trends Plant Sci. 9 (2004) 229–235.
[4] J. Mansfeld, Plant phospholipases A2: perspectives on biotechnological applications, Biotechnol. Lett. 31 (2009) 1373–1380.
[5] L. De Maria, J. Vind, K.M. Oxenbøll, A. Svendsen, S. Patkar, Phospholipases and their industrial applications, Appl. Microbiol. Biotechnol. 74 (2007) 290–300.
[6] G.S. Richmond, T.K. Smith, Phospholipases A1, Int. J. Mol. Sci. 12 (2011) 588–612.
[7] Y. Hyun, S. Choi, H.J. Hwang, J. Yu, S.J. Nam, J. Ko, J.Y. Park, Y.S. Seo, E.Y. Kim, S.B. Ryu, W.T. Kim, Y.H. Lee, H. Kang, I. Lee, Cooperation and functional diversification of two closely related galactolipase genes for jasmonate biosynthesis, Dev. Cell 14 (2008) 183–192.
[8] S. Ishiguro, A. Kawai-Oda, J. Ueda, I. Nishida, K. Okada, The DEFECTIVE IN ANTHER DEHISCENCE1 gene encodes a novel phospholipase A1 catalyzing the initial step of jasmonic acid biosynthesis, which synchronizes pollen maturation, anther dehiscence, and flower opening in Arabidopsis, Plant Cell 13 (2001) 2191–2209.
[9] M. Lo, C. Taylor, L. Wang, L. Nowack, T.-W. Wang, J. Thompson, Characterization of an ultraviolet B-induced lipase in Arabidopsis, Plant Physiol. 135 (2004) 947–958.
[10] Y.S. Seo, E.Y. Kim, H.G. Mang, W.T. Kim, Heterologous expression, and biochemical and cellular characterization of CaPLA1 encoding a hot pepper phospholipase A1 homolog: hot pepper phospholipase A1, Plant J. 53 (2007) 895–908.
[11] Y. Hong, T.-W. Wang, K.A. Hudak, F. Schade, C.D. Froese, J.E. Thompson, An ethylene-induced cDNA encoding a lipase expressed at the onset of senescence, Proc. Natl. Acad. Sci. 97 (2000) 8717–8722.
[12] A. Noiriel, P. Benveniste, A. Banas, S. Stymne, P. Bouvier-Navé, Expression in yeast of a novel phospholipase A1 cDNA from Arabidopsis thaliana, Eur. J. Biochem. 271 (2004) 3752–3764.
[13] T. Kato, M.T. Morita, H. Fukaki, Y. Yamauchi, M. Uehara, M. Niihama, M. Tasaka, SGR2, a phospholipase-like protein, and ZIG/SGR4, a SNARE, are involved in the shoot gravitropism of Arabidopsis, Plant Cell 14 (2002) 33–46.
[14] K. Matsui, S. Fukutomi, M. Ishii, T. Kajiwara, A tomato *lipase homologous to DAD1* (*LeLID1*) is induced in post-germinative growing stage and encodes a triacylglycerol lipase, FEBS Lett. 569 (2004) 195–200.
[15] A.R. Matos, A.-T. Pham-Thi, Lipid deacylating enzymes in plants: old activities, new genes, Plant Physiol. Biochem. 47 (2009) 491–503.
[16] Y.S. Seo, E.Y. Kim, J.H. Kim, W.T. Kim, Enzymatic characterization of class I DAD1-like acylhydrolase members targeted to chloroplast in Arabidopsis, FEBS Lett. 583 (2009) 2301–2307.
[17] Y. Li-Beisson, B. Shorrosh, F. Beisson, M.X. Andersson, V. Arondel, P.D. Bates, S. Baud, D. Bird, A. DeBono, T.P. Durrett, R.B. Franke, I.A. Graham, K. Katayama, A.A. Kelly, T. Larson, J.E. Markham, M. Miquel, I. Molina, I. Nishida, O. Rowland, L. Samuels, K.M. Schmid, H. Wada, R. Welti, C. Xu, R. Zallot, J. Ohlrogge, Acyl-Lipid Metabolism, The Arabidopsis Book, (2013).
[18] L. Casas-Godoy, S. Duquesne, F. Bordes, G. Sandoval, A. Marty, Lipases: an overview, in: G. Sandoval (Ed.), Lipases and Phospholipases, Humana Press, Totowa, NJ, 2012, pp. 3–30.

[19] J. Pleiss, M. Fischer, M. Peiker, C. Thiele, R.D. Schmid, Lipase Engineering Database Understanding and Exploiting Sequence–Structure–Function Relationships, (2000), p. 18.

[20] I. Ruduś, H. Terai, T. Shimizu, H. Kojima, K. Hattori, Y. Nishimori, H. Tsukagoshi, Y. Kamiya, M. Seo, K. Nakamura, J. Kepczyński, S. Ishiguro, Wound-induced expression of DEFECTIVE IN ANTHER DEHISCENCE1 and DAD1-like lipase genes is mediated by both CORONATINE INSENSITIVE1-dependent and independent pathways in Arabidopsis thaliana, Plant Cell Rep. 33 (2014) 849–860.

[21] D. Ellinger, N. Stingl, I.I. Kubigsteltig, T. Bals, M. Juenger, S. Pollmann, S. Berger, D. Schuenemann, M.J. Mueller, DONGLE and DEFECTIVE IN ANTHER DEHISCENCE1 lipases are not essential for wound- and pathogen-induced jasmonate biosynthesis: redundant lipases contribute to jasmonate formation, Plant Physiol. 153 (2010) 114–127.

[22] D. Ellinger, I.I. Kubigsteltig, Involvement of DAD1-like lipases in response to salt and osmotic stress in *Arabidopsis thaliana*, Plant Signal. Behav. 5 (2010) 1269–1271.

[23] M. Sato, R.M. Mitra, J. Coller, D. Wang, N.W. Spivey, J. Dewdney, C. Denoux, J. Glazebrook, F. Katagiri, A high-performance, small-scale microarray for expression profiling of many samples in Arabidopsis-pathogen studies, Plant J. 49 (2007) 565–577.

[24] A. Agalou, H.P. Spaink, A. Roussis, Novel interaction of selenium-binding protein with glyceraldehyde-3-phosphate dehydrogenase and fructose-bisphosphate aldolase of Arabidopsis thaliana, Funct. Plant Biol. 33 (2006) 847.

[25] R. Desikan, S.A.-H. Mackerness, J.T. Hancock, S.J. Neill, Regulation of the Arabidopsis transcriptome by oxidative stress, Plant Physiol. 127 (2001) 159–172.

[26] V. Nikiforova, J. Freitag, S. Kempa, M. Adamik, H. Hesse, R. Hoefgen, Transcriptome analysis of sulfur depletion in *Arabidopsis thaliana* : interlacing of biosynthetic pathways provides response specificity, Plant J. 33 (2003) 633–650.

[27] X. Liu, W.V. Baird, Differential expression of genes regulated in response to drought or salinity stress in Sunflower, Crop Sci. 43 (2003) 10.

[28] Y. Zhao, A.K. Hull, N.R. Gupta, K.A. Goss, J. Alonso, J.R. Ecker, J. Normanly, J. Chory, J.L. Celenza, Trp-dependent auxin biosynthesis in Arabidopsis: involvement of cytochrome P450s CYP79B2 and CYP79B3, Genes Dev. 16 (2002) 3100–3112.

[29] K. Zhu-Salzman, Ra. Salzman, J.-E. Ahn, H. Koiwa, Transcriptional regulation of sorghum defense determinants against a phloem-feeding aphid, Plant Physiol. 134 (2004) 420–431.

[30] K. Sawada, M. Iwata, Isolation of blast fungal cerebroside elicitor-responsive genes in rice plants, J. Gen. Plant Pathol. 68 (2002) 128–133.

[31] K. Sawada, L. Tokuda, A. Shinmy, Characterization of the rice blast fungal elicitor-responsive gene OsSBP encoding a homolog to the mammalian Selenium-binding Protelns, Plant Biotechnol. 20 (2003) 177–181.

[32] K. Sawada, M. Hasegawa, L. Tokuda, J. Kameyama, O. Kodama, T. Kohchi, K. Yoshida, A. Shinmyo, Enhanced resistance to blast fungus and bacterial blight in transgenic rice constitutively expressing *OsSBP*, a rice homologue of mammalian Selenium-binding Proteins, Biosci. Biotechnol. Biochem. 68 (2004) 873–880.

[33] C. Valassakis, I. Dervisi, A. Agalou, N. Papandreou, G. Kapetsis, V. Podia, K. Haralampidis, V.A. Iconomidou, H.P. Spaink, A. Roussis, Novel interactions of Selenium Binding Protein family with the PICOT containing proteins AtGRXS14 and AtGRXS16 in Arabidopsis thaliana, Plant Sci. 281 (2019) 102–112.

[34] C. Valassakis, P. Livanos, M. Minopetrou, K. Haralampidis, A. Roussis, Promoter analysis and functional implications of the selenium binding protein (SBP) gene family in Arabidopsis thaliana, J. Plant Physiol. 224–225 (2018) 19–29.

[35] T. Murashige, F. Skoog, A revised medium for rapid growth and bioassays with tobacco tissue cultures, Physiol. Plant. 15 (1962) 473–497.

[36] L. Oñate-Sánchez, J. Vicente-Carbajosa, DNA-free RNA isolation protocols for *Arabidopsis thaliana*, including seeds and siliques, BMC Res. Notes 1 (2008) 93.

[37] K.J. Livak, T.D. Schmittgen, Analysis of relative gene expression data using Real-Time Quantitative PCR and the $2^{-\Delta\Delta CT}$ Method, Methods. 25 (2001) 402–408.

[38] G. An, P.R. Ebert, A. Mitra, S.B. Ha, Binary vectors, in: S.B. Gelvin, R.A. Schilperoort, D.P.S. Verma (Eds.), Plant Molecular Biology Manual, Springer, Dordrecht, 1989, pp. 29–47.

[39] A.M. Davis, A. Hall, A.J. Millar, C. Darrah, S.J. Davis, Protocol: streamlined sub-protocols for floral-dip transformation and selection of transformants in *Arabidopsis thaliana*, Plant Methods 5 (2009) 3.

[40] R.A. Jefferson, T.A. Kavanagh, M.W. Bevan, GUS fusions: beta-glucuronidase as a sensitive and versatile gene fusion marker in higher plants, EMBO J. 6 (1987) 3901–3907.

[41] S.R. Gallagher, Quantitation of GUS activity by fluorometry, in: S.R. Gallagher (Ed.), Gus Protocols: Using the GUS Gene as a Reporter Gene of Gene Expression, Academic Press Inc, California, 1992, pp. 47–59.

[42] M.M. Bradford, A rapid and sensitive method for the quantitation of microgram quantities of protein utilizing the principle of protein-dye binding, Anal. Biochem. 72 (1976) 248–254.

[43] F.-H. Wu, S.-C. Shen, L.-Y. Lee, S.-H. Lee, M.-T. Chan, C.-S. Lin, Tape-Arabidopsis Sandwich - a simpler Arabidopsis protoplast isolation method, Plant Methods 5 (2009) 10.

[44] B.O.R. Bargmann, K.D. Birnbaum, Fluorescence activated cell sorting of plant protoplasts, J. Vis. Exp. (2010) 1673.

[45] L. Brady, A.M. Brzozowski, Z. Derewenda, E. Dodson, G. Dodson, S. Tolley, J.P. Turkenburg, L. Christiansen, B. Huge-Jensen, L. Norskov, L. Thim, U. Menge, A serine protease triad forms the catalytic centre of triacylglyceol lipase, Lett. Nature. 343 (1990) 767–770.

[46] D.L. Sworffor, PAUP*. Phylogenetic Analysis Using Parsimony (*and Other Methods), Version 4, Sinauer Associates, Sunderland, Massachusetts, 2002.

[47] R. Lanfear, B. Calcott, S.Y.W. Ho, S. Guindon, PartitionFinder: Combined selection of partitioning schemes and substitution models for phylogenetic analyses, Mol. Biol. Evol. 29 (2012) 1695–1701.

[48] R. Lanfear, P.B. Frandsen, A.M. Wright, T. Senfeld, B. Calcott, PartitionFinder 2: new methods for selecting partitioned models of evolution for molecular and morphological phylogenetic analyses, Mol. Biol. Evol. (2016) 772–773.

[49] S. Guindon, J.-F. Dufayard, V. Lefort, M. Anisimova, W. Hordijk, O. Gascuel, New algorithms and methods to estimate Maximum-Likelihood Phylogenies: assessing the performance of PhyML 3.0, Syst. Biol. 59 (2010) 307–321.

[50] F. Ronquist, M. Teslenko, P. van der Mark, D.L. Ayres, A. Darling, S. Höhna, B. Larget, L. Liu, M.A. Suchard, J.P. Huelsenbeck, MrBayes 3.2: efficient Bayesian Phylogenetic inference and Model choice across a large model space, Syst. Biol. 61 (2012) 539–542.

[51] A. Gelman, D.B. Rubin, Inference from iterative simulation using multiple sequences, Stat. Sci. 7 (1992) 457–511.

[52] B.C. Stöver, K.F. Müller, TreeGraph 2: combining and visualizing evidence from different phylogenetic analyses, BMC Bioinformatics 11 (2010).

[53] A. Roy, A. Kucukural, Y. Zhang, I-TASSER: a unified platform for automated protein structure and function prediction, Nat. Protoc. 5 (2010) 725–738.

[54] J. Yang, R. Yan, A. Roy, D. Xu, J. Poisson, Y. Zhang, The I-TASSER Suite: protein structure and function prediction, Nat. Methods 12 (2015) 7–8.

[55] The UniProt Consortium, UniProt: the universal protein knowledgebase, Nucleic Acids Res. 46 (2018) 2699.

[56] J. Yang, A. Roy, Y. Zhang, Protein–ligand binding site recognition using complementary binding-specific substructure comparison and sequence profile alignment, Bioinformatics. 29 (2013) 2588–2595.

[57] M.J. Abraham, T. Murtola, R. Schulz, S. Páll, J.C. Smith, B. Hess, E. Lindahl, GROMACS: High performance molecular simulations through multi-level parallelism from laptops to supercomputers, SoftwareX 1–2 (2015) 19–25.

[58] K. Lindorff-Larsen, S. Piana, K. Palmo, P. Maragakis, J.L. Klepeis, R.O. Dror, D.E. Shaw, Improved side-chain torsion potentials for the Amber ff99SB protein force field, Proteins 78 (2010) 1950–1958.

[59] M. Nardini, B.W. Dijkstra, A/β Hydrolase fold enzymes: the family keeps growing, Curr. Opin. Struct. Biol. 9 (1999) 732–737.

[60] J.T. Mindrebo, C.M. Nartey, Y. Seto, M.D. Burkart, J.P. Noel, Unveiling the functional diversity of the alpha/beta hydrolase superfamily in the plant kingdom, Curr. Opin. Struct. Biol. 41 (2016) 233–246.

[61] H.-P. Klenk, R.A. Clayton, J.-F. Tomb, O. White, K.E. Nelson, K.A. Ketchum, R.J. Dodson, M. Gwinn, E.K. Hickey, J.D. Peterson, D.L. Richardson, A.R. Kerlavage, D.E. Graham, N.C. Kyrpides, R.D. Fleischmann, J. Quackenbush, N.H. Lee, G.G. Sutton, S. Gill, E.F. Kirkness, B.A. Dougherty, K. McKenney, M.D. Adams, B. Loftus, S. Peterson, C.I. Reich, L.K. McNeil, J.H. Badger, A. Glodek, L. Zhou, R. Overbeek, J.D. Gocayne, J.F. Weidman, L. McDonald, T. Utterback, M.D. Cotton, T. Spriggs, P. Artiach, B.P. Kaine, S.M. Sykes, P.W. Sadow, K.P. D'Andrea, C. Bowman, C. Fujii, S.A. Garland, T.M. Mason, G.J. Olsen, C.M. Fraser, H.O. Smith, C.R. Woese, J.C. Venter, The complete genome sequence of the hyperthermophilic, sulphate-reducing archaeon Archaeoglobus fulgidus, Nature 390 (1997) 364–370.

[62] G. De Simone, V. Menchise, G. Manco, L. Mandrich, N. Sorrentino, D. Lang, M. Rossi, C. Pedone, The Crystal structure of a hyper-thermophilic carboxylesterase from the archaeon Archaeoglobus fulgidus, J. Mol. Biol. 314 (2001) 507–518.

[63] F.K. Winkler, A. D'Arcy, W. Hunziker, Structure of human pancreatic lipase, Nature 343 (1990) 771–774.

[64] F. Carrière, C. Withers-Martinez, H. van Tilbeurgh, A. Roussel, C. Cambillau, R. Verger, Structural basis for the substrate selectivity of pancreatic lipases and some related proteins, Biochim. Biophys. Acta Biomembr. 1376 (1998) 417–432.

[65] A.M. Brzozowski, H. Savage, C.S. Verma, J.P. Turkenburg, D.M. Lawson, A. Svendsen, S. Patkar, Structural origins of the interfacial activation in *Thermomyces* (*Humicola*) *lanuginosa* Lipase, Biochemistry 39 (2000) 15071–15082.

[66] Z.S. Derewenda, U. Derewenda, Relationships among serine hydrolases: evidence for a common structural motif in triacylglyceride lipases and esterases, Biochem. Cell Biol. 69 (1991) 842–851.

[67] P. Grochulski, Y. Li, F. Bouthillier, P. Smith, D. Harrison, B. Rubin, M. Cygler, Insights into interfacial activation from an "open" structure of *Candida rugosa* lipase, J. Biol. Chem. 268 (1993) 12843–12847.

[68] P. Grochulski, Y. Li, J.D. Schrag, M. Cygler, Two conformational states of *Candida rugosa* lipase, Prot. Sci. 3 (1993) 82–91.

[69] Z.S. Derewenda, U. Derewenda, G.G. Dodson, The crystal and molecular structure of the *Rhizomucor miehei* triacylglyceride lipase at 1.9Å resolution, J. Mol. Biol. 227 (1992) 818–839.

[70] N.L. Dawson, T.E. Lewis, S. Das, J.G. Lees, D. Lee, P. Ashford, C.A. Orengo, I. Sillitoe, CATH: an expanded resource to predict protein function through structure and sequence, Nucleic Acids Res. 45 (2017) D289–D295.

[71] H.M. Berman, J. Westbrook, Z. Feng, G. Gilliland, T.N. Bhat, H. Weissig, I.N. Shindyalov, P.E. Bourne, The protein data bank, Nucleic Acids Res. 28 (2000) 235–242.

[72] C.A. Orengo, W.R. Taylor, [36] SSAP: Sequence structure alignment program for protein structure comparison, Methods Enzymol. 226 (1996) 617–635.

[73] N.K. Fox, S.E. Brenner, J.-M. Chandonia, SCOPe: Structural Classification of Proteins—extended, integrating SCOP and ASTRAL data and classification of new structures, Nucl. Acids Res. 42 (2014) D304–D309.

[74] J.A. Banks, Selaginella and 400 million years of separation, Annu. Rev. Plant Biol. 60 (2009) 223–238.

[75] J.A. Banks, T. Nishiyama, M. Hasebe, J.L. Bowman, M. Gribskov, C. dePamphilis, V.A. Albert, N. Aono, T. Aoyama, B.A. Ambrose, N.W. Ashton, M.J. Axtell, E. Barker, M.S. Barker, J.L. Bennetzen, N.D. Bonawitz, C. Chapple, C. Cheng,

L.G.G. Correa, M. Dacre, J. DeBarry, I. Dreyer, M. Elias, E.M. Engstrom, M. Estelle, L. Feng, C. Finet, S.K. Floyd, W.B. Frommer, T. Fujita, L. Gramzow, M. Gutensohn, J. Harholt, M. Hattori, A. Heyl, T. Hirai, Y. Hiwatashi, M. Ishikawa, M. Iwata, K.G. Karol, B. Koehler, U. Kolukisaoglu, M. Kubo, T. Kurata, S. Lalonde, K. Li, Y. Li, A. Litt, E. Lyons, G. Manning, T. Maruyama, T.P. Michael, K. Mikami, S. Miyazaki, S.-i. Morinaga, T. Murata, B. Mueller-Roeber, D.R. Nelson, M. Obara, Y. Oguri, R.G. Olmstead, N. Onodera, B.L. Petersen, B. Pils, M. Prigge, S.A. Rensing, D.M. Riano-Pachon, A.W. Roberts, Y. Sato, H.V. Scheller, B. Schulz, C. Schulz, E.V. Shakirov, N. Shibagaki, N. Shinohara, D.E. Shippen, I. Sorensen, R. Sotooka, N. Sugimoto, M. Sugita, N. Sumikawa, M. Tanurdzic, G. Theissen, P. Ulvskov, S. Wakazuki, J.-K. Weng, W.W.G.T. Willats, D. Wipf, P.G. Wolf, L. Yang, A.D. Zimmer, Q. Zhu, T. Mitros, U. Hellsten, D. Loque, R. Otillar, A. Salamov, J. Schmutz, H. Shapiro, E. Lindquist, S. Lucas, D. Rokhsar, I.V. Grigoriev, The Selaginella genome identifies genetic changes associated with the evolution of vascular plants, Science. 332 (2011) 960–963.

[76] Y.S. Seo, E.Y. Kim, W.T. Kim, The *Arabidopsis sn*-1-specific mitochondrial acyl-hydrolase AtDLAH is positively correlated with seed viability, J. Exp. Bot. 62 (2011) 5683–5698.

[77] C. Dutilleul, A. Jourdain, J. Bourguignon, V. Hugouvieux, The Arabidopsis Putative Selenium-Binding Protein Family: expression study and characterization of SBP1 as a potential new player in cadmium detoxification processes, Plant Physiol. 147 (2008) 239–251.

[78] J.-E. Sarry, L. Kuhn, C. Ducruix, A. Lafaye, C. Junot, V. Hugouvieux, A. Jourdain, O. Bastien, J.B. Fievet, D. Vailhen, B. Amekraz, C. Moulin, E. Ezan, J. Garin, J. Bourguignon, The early responses of *Arabidopsis thaliana* cells to cadmium exposure explored by protein and metabolite profiling analyses, Proteomics 6 (2006) 2180–2198.

[79] U.-H. Cho, N.-H. Seo, Oxidative stress in *Arabidopsis thaliana* exposed to cadmium is due to hydrogen peroxide accumulation, Plant Sci. 168 (2005) 113–120.

[80] R.G. Upchurch, Fatty acid unsaturation, mobilization, and regulation in the response of plants to stress, Biotechnol. Lett. 30 (2008) 967–977.

[81] L. Yang, J. Ji, K.R. Harris-Shultz, H. Wang, H. Wang, E.F. Abd-Allah, Y. Luo, X. Hu, The dynamic changes of the plasma membrane proteins and the protective roles of nitric oxide in rice subjected to heavy metal cadmium stress, Front. Plant Sci. 7 (2016).

[82] J. Chmielowska-Bąk, J. Gzyl, R. Rucinska-Sobkowiak, M. Arasimowicz-Jelonek, J. Deckert, The new insights into cadmium sensing, Front. Plant Sci. 5 (2014).

[83] W. Maksymiec, D. Wianowska, A.L. Dawidowicz, S. Radkiewicz, M. Mardarowicz, Z. Krupa, The level of jasmonic acid in *Arabidopsis thaliana* and *Phaseolus coccineus* plants under heavy metal stress, J. Plant Physiol. 162 (2005) 1338–1346.

[84] W. Maksymiec, Signaling responses in plants to heavy metal stress, Acta Physiol. Plant. 29 (2007) 177–187.

[85] T. Koeduka, K. Matsui, M. Hasegawa, Y. Akakabe, T. Kajiwara, Rice fatty acid -dioxygenase is induced by pathogen attack and heavy metal stress: activation through jasmonate signaling, J. Plant Physiol. 162 (2005) 912–920.

[86] A. Mithöfer, B. Schulze, W. Boland, Biotic and heavy metal stress response in plants: evidence for common signals, FEBS Lett. 566 (2004) 1–5.

[87] W. Maksymiec, Effects of jasmonate and some other signalling factors on bean and onion growth during the initial phase of cadmium action, Biol. Plant. 55 (2011) 112–118.

[88] Z. Zhang, D.B. Collinge, H. Thordal-Christensen, Germin-like oxalate oxidase, a H_2O_2-producing enzyme, accumulates in barley attacked by the powdery mildew fungus, Plant J. 8 (1995) 139–145.

[89] G.M. Pastori, C.H. Foyer, Common components, networks, and pathways of cross-tolerance to stress. The central role of “Redox” and abscisic acid-mediated controls, Plant Physiol. 129 (2002) 460–468.

[90] K.R. Atkuri, J.J. Mantovani, L.A. Herzenberg, L.A. Herzenberg, N-Acetylcysteine—a safe antidote for cysteine/glutathione deficiency, Curr. Opin. Pharmacol. 7 (2007) 355–359.

[91] A.M. Sadowska, B. Manuel-Y-Keenoy, W.A. De Backer, Antioxidant and anti-inflammatory efficacy of NAC in the treatment of COPD: discordant in vitro and in vivo dose-effects: a review, Pulm. Pharmacol. Ther. 20 (2007) 9–22.

[92] W.R. Swindell, The association among gene expression responses to nine abiotic stress treatments in Arabidopsis thaliana, Genetics 174 (2006) 1811–1824.

[93] Y.H. Cheong, H.-S. Chang, R. Gupta, X. Wang, T. Zhu, S. Luan, Transcriptional profiling reveals novel interactions between wounding, pathogen, abiotic stress, and hormonal responses in Arabidopsis, Plant Physiol. 129 (2002) 661–677.

[94] H. Candela, A. Martínez-Laborda, J. Luis Micol, Venation pattern formation in *Arabidopsis thaliana* vegetative leaves, Dev. Biol. 205 (1999) 205–216.

[95] R. Aloni, K. Schwalm, M. Langhans, C.I. Ullrich, Gradual shifts in sites of free-auxin production during leaf-primordium development and their role in vascular differentiation and leaf morphogenesis in Arabidopsis, Planta 213 (2003) 841–853.

[96] H. Yi, D. Park, Y. Lee, In vivo evidence for the involvement of phospholipase A and protein kinase in the signal transduction pathway for auxin-induced corn coleoptile elongation, Physiol. Plant. 96 (1996) 359–368.

[97] G.F.E. Scherer, M. Zahn, J. Callis, A.M. Jones, A role for phospholipase A in auxin-regulated gene expression, FEBS Lett. 581 (2007) 4205–4211.

[98] R.U. Paul, A. Holk, G.F.E. Scherer, Fatty acids and lysophospholipids as potential second messengers in auxin action. Rapid activation of phospholipase A2 activity by auxin in suspension-cultured parsley and soybean cells, Plant J. 16 (1998) 601–611.

[99] C. Labusch, M. Shishova, Y. Effendi, M. Li, X. Wang, G.F.E. Scherer, Patterns and timing in expression of early auxin-induced genes imply involvement of phospholipases A (pPLAs) in the regulation of auxin responses, Mol. Plant 6 (2013) 1473–1486.

[100] R. Ghelli, P. Brunetti, N. Napoli, A. De Paolis, V. Cecchetti, T. Tsuge, G. Serino, M. Matsui, G. Mele, G. Rinaldi, G.A. Palumbo, F. Barozzi, P. Costantino, M. Cardarelli, A newly identified flower-specific splice variant of AUXIN RESPONSE FACTOR8 regulates stamen elongation and endothecium lignification in Arabidopsis, Plant Cell 30 (2018) 620–637.

[101] R. Tabata, M. Ikezaki, T. Fujibe, M. Aida, C. Tian, Y. Ueno, K.T. Yamamoto, Y. Machida, K. Nakamura, S. Ishiguro, Arabidopsis AUXIN RESPONSE FACTOR6 and 8 regulate jasmonic acid biosynthesis and floral organ development via repression of class 1 KNOX genes, Plant Cell Physiol. 51 (2010) 164–175.

[102] P. Nagpal, C.M. Ellis, H. Weber, S.E. Ploense, L.S. Barkawi, T.J. Guilfoyle, G. Hagen, J.M. Alonso, J.D. Cohen, E.E. Farmer, J.R. Ecker, J.W. Reed, Auxin response factors ARF6 and ARF8 promote jasmonic acid production and flower maturation, Development. 132 (2005) 4107–4118.

[103] E. Grienenberger, P. Geoffroy, J. Mutterer, M. Legrand, T. Heitz, The interplay of lipid acyl hydrolases in inducible plant defense, Plant Signal. Behav. 5 (2010) 1181–1186.

[104] I.M.A. Nooren, J.M. Thornton, Diversity of protein-protein interactions, EMBO J. 22 (2003) 3486–3492.

[105] G. Chen, H. Wang, C.T. Miller, D.G. Thomas, T.G. Gharib, D.E. Misek, T.J. Giordano, M.B. Orringer, S.M. Hanash, D.G. Beer, Reduced Selenium-Binding Protein 1 expression is associated with poor outcome in lung adenocarcinomas, J. Pathol. 202 (2004) 321–329.

[106] J.-Y. Jeong, Y. Wang, A.J. Sytkowski, Human Selenium Binding Protein-1 (hSP56) interacts with VDU1 in a selenium-dependent manner, Biochem. Biophys. Res. Commun. 379 (2009) 583–588.

[107] P.W.G. Chang, S.K.W. Tsui, C. Liew, C. Lee, M.M.Y. Waye, K. Fung, Isolation, characterization, and chromosomal mapping of a novel cDNA clone encoding human selenium binding protein, J. Cell. Biochem. 64 (1997) 217–224.

[108] E. Flemetakis, A. Agalou, N. Kavroulakis, M. Dimou, A. Martsikovskaya, A. Slater, H.P. Spaink, A. Roussis, P. Katinakis, *Lotus japonicus* gene *Ljsbp* is highly conserved among plants and animals and encodes a homologue to the mammalian Selenium-Binding Proteins, Mol. Plant Microbe Interact. 15 (2002) 313–322.

[109] L.-Y. Lee, M.-J. Fang, L.-Y. Kuang, S.B. Gelvin, Vectors for multi-color bimolecular fluorescence complementation to investigate protein-protein interactions in living plant cells, Plant Methods 4 (2008) 24.

[110] T.K. Kerppola, Bimolecular Fluorescence Complementation (BiFC) analysis as a probe of protein interactions in living cells, Annu. Rev. Biophys. 37 (2008) 465–487.

[111] V. Citovsky, L.-Y. Lee, S. Vyas, E. Glick, M.-H. Chen, A. Vainstein, Y. Gafni, S.B. Gelvin, T. Tzfira, Subcellular localization of interacting proteins by Bimolecular Fluorescence Complementation *in planta*, J. Mol. Biol. 362 (2006) 1120–1131.

[112] A.B. Machettira, L.E. Groß, B. Tillmann, B.L. Weis, G. Englich, M.S. Sommer, M. Königer, E. Schleiff, Protein-induced modulation of chloroplast membrane morphology, Front. Plant Sci. 2 (2012).

[113] N.J. Ruppel, C.A. Logsdon, C.W. Whippo, K. Inoue, R.P. Hangarter, A Mutation in Arabidopsis SEEDLING PLASTID DEVELOPMENT1 affects plastid differentiation in embryo-derived tissues during seedling growth, Plant Physiol. 155 (2011) 342–353.

[114] S. Wan, M.-W. Mak, S.-Y. Kung, Ensemble linear neighborhood propagation for predicting subchloroplast localization of multi-location proteins, J. Proteome Res. 15 (2016) 4755–4762.